

BERTology of Molecular Property Prediction

Mohammad Mostafanejad,^{*,†,‡} Paul Saxe,^{*,†,‡} and T. Daniel Crawford^{*,†,‡}

[†]*Department of Chemistry, Virginia Tech, Blacksburg, Virginia 24061, USA*

[‡]*Molecular Sciences Software Institute, Blacksburg, Virginia 24060, USA*

E-mail: smostafanejad@vt.edu; psaxe@vt.edu; crawdad@vt.edu

Abstract

Chemical language models (CLMs) have emerged as promising competitors to popular classical machine learning models for molecular property prediction (MPP) tasks. However, an increasing number of studies have reported inconsistent and contradictory results for the performance of CLMs across various MPP benchmark tasks. In this study, we conduct and analyze hundreds of meticulously controlled experiments to systematically investigate the effects of various factors, such as dataset size, model size, and standardization, on the pre-training and fine-tuning performance of CLMs for MPP. In the absence of well-established scaling laws for encoder-only masked language models, our aim is to provide comprehensive numerical evidence and a deeper understanding of the underlying mechanisms affecting the performance of CLMs for MPP tasks, some of which appear to be entirely overlooked in the literature.

Molecular property prediction (MPP) is a fundamental task in materials design and drug discovery campaigns which involves using computational models to predict the physicochemical properties of chemical compounds from their molecular features.¹⁻⁴ In order to be able to significantly accelerate the computational simulations and reduce the cost of experimental procedures in discovery workflows, MPP models should overcome two major challenges:⁵ the scarcity of large-scale high-quality annotated datasets in chemistry,⁶ and the complexity of

finding an effective molecular representation that can capture the underlying physicochemical phenomena governing the target properties.¹⁻⁴

For decades, classical machine learning (ML) models have been widely used for MPP tasks, where the molecular structures are represented using expert-engineered molecular descriptors. However, the presence of label noise, the absence of standardization and the lack of expertise in feature engineering can harm the generalization capabilities of the models.^{2,7} Alternatively, feed-forward neural networks⁸ can learn complex molecular features directly from the data. Nonetheless, they often require large amounts of labeled data for training and can be prone to overfitting.

Recent advances in natural language processing (NLP), especially the introduction of Transformers,⁹ have contributed to the development of chemical language models (CLMs) for MPP tasks. Transformers treat the textual representations of molecules, such as Simplified Molecular Input Line Entry System (SMILES),¹⁰ as the language of chemistry and learn its underlying structure, rules, syntax and semantics via language modeling objectives. Although Transformers are extremely effective in parallel processing of long-range dependencies in sequences, they are limited by their uni-directional left-to-right self-attention¹¹ and auto-regressive training objectives.

The aforementioned limitation of Transformer architecture sparked the development of Bidirectional Encoder Representations from Transformers (BERT)¹² along with a two-step self-supervised learning (SSL) paradigm which promotes the training of deep bidirectional encoder-only models for language understanding tasks. The SSL begins with training a large language model (LLM) on a vast corpus of unlabeled data to learn the underlying structure and semantics of the language at a high level. The pre-trained foundation model is then fine-tuned on a smaller annotated dataset to adapt its learned representations towards specific requirements of the downstream task.¹² The fine-tuned models can then be converted into small language models (SLMs) using compression and optimization techniques such as knowledge distillation,¹³ pruning and quantization to improve their computational efficiency and

reduce their memory requirements for deployment in resource-constrained environments.^{14,15}

The success of BERT in NLP has inspired the development of a slew of CLMs for MPP.¹⁶⁻³¹ However, an increasing number of studies involving CLMs have reported performance results that are inconsistent and contradictory across various MPP benchmark tasks. For instance, several recent studies^{25,28,32} reported that the performance of multiple BERT-based CLMs for MPP tasks can deteriorate as the size of the pre-training dataset increases. Other similar cases have been documented in a recent review.³³

The scaling laws of LLMs establish an empirical power-law relation between the testing performance of auto-regressive language models and factors such as the model size, dataset size and the amount of compute used for training.^{34,35} Nevertheless, to our knowledge, there is no rigorous framework that extends the scaling laws to encoder-only models with masked language modeling (MLM) objective. As such, in a quest to find the source of reported inconsistencies in the literature, we resort to conducting hundreds of carefully controlled experiments to systematically explore the impact of elements such as dataset size, model size, tokenization, model architecture and standardization on the pre-training and fine-tuning performance of CLMs for MPP. Through this study, we aim to provide a comprehensive understanding of the underlying mechanisms, backed by numerical evidence, to shed light on factors that appear to be entirely overlooked in the literature.

Results

In the following sections, we investigate the impact of a variety of factors on the pre-training and fine-tuning performance of BERT. Throughout our analysis, two aspects will frequently come up: the model size and the dataset size. This is intentional, as we intend to provide evidence pertinent to the scaling laws of LLMs with MLM objective and demonstrate that the observed numerical trends remain consistent across all studied experimental settings.

Model Initialization and Data Sampling Randomness in Pre-training

Randomness is an inherent part of the pre-training process but seldom receives much attention in the MPP literature. We assess the variability of the pre-training performance of BERT variants with respect to the model weight initialization and data sampling randomness. For each model variant, we perform five independent experiments over 10 epochs with different random seeds. All pre-training runs use the entire 119,184,806 canonical stereoisomeric SMILES entries in the PubChem dataset which is randomly split into 95,347,844 data points ($\sim 80\%$ of the data) for training and 23,836,962 data points for validation ($\sim 20\%$ of the data) sets. The average pre-training performance metrics, defined in Methods, are reported in Table 1.

Table 1: Variations of the averaged pre-training performance metrics with 95% confidence intervals^a for masked language modeling with respect to the model weight initialization and data sampling seeds

BERT Variant	T-Loss \downarrow^c	V-Loss \downarrow^c	V-Acc \uparrow^c	V-wF1 \uparrow^c	V-PPPL \downarrow^c
Tiny	0.6511 ± 0.0090	0.4696 ± 0.0053	0.8823 ± 0.0077	0.8686 ± 0.0085	1.5993 ± 0.0085
Small	0.2353 ± 0.0009	0.1836 ± 0.0008	0.9453 ± 0.0109	0.9412 ± 0.0116	1.2016 ± 0.0010
Base^b	0.1779 ± 0.0006	0.1359 ± 0.0011	0.9595 ± 0.0046	0.9564 ± 0.0041	1.1455 ± 0.0013

^a The statistical summaries ($\bar{x} \pm (s_N/\sqrt{N})t_{95\%,N-1}$) for each performance metric is calculated over five runs with different data sampling and model initialization seeds. The critical value of the two-sided t -distribution with 95% confidence interval is taken from Ref. 36.

^b A diverged model training session was excluded from the mean and standard deviation calculations which persisted over several runs. For more details, see the Table 1 in the Extended Data.

^c \uparrow : higher is better; \downarrow : lower is better.

The results in Table 1 demonstrate that the variations in the performance of the models, due to randomness in data sampling and model initialization, are small ($\approx 1\%$) compared to those caused by the model size. Specifically, increasing the model size from Tiny-BERT to Base-BERT decreases the average training (validation) loss values from 0.6511 ± 0.0090 (0.4696 ± 0.0053) to 0.1779 ± 0.0006 (0.1359 ± 0.0011) by $>70\%$, decreases the average pseudo-perplexity (V-PPPL) values by more than 28% from 1.5993 ± 0.0085 to $1.1455 \pm$

0.0013, and increases the average validation accuracy, V-Acc, (weighted-F1 score, V-wF1) by more than 8% from 0.8823 ± 0.0077 (0.8686 ± 0.0085) to 0.9595 ± 0.0046 (0.9564 ± 0.0041), respectively.

Standardization Effects on Pre-training

We hypothesize that combining SMILES from different chemical databases may amount to mixing different standardization protocols which can confuse the model during pre-training and lead to degraded performance. In order to simulate the impact of standardization noise on the pre-training performance of BERT, we gradually replace various percentages of the PubChem SMILES in the training and validation splits with their corresponding ChEMBL-standardized counterparts. The SMILES corruption percentages in the training and validation splits are controlled by the parameters τ and ν , respectively (Fig. 1) according to the recipe, described in the Supporting Information. Briefly, the standardization noise in the training split can change between pure PubChem ($\tau=0$) and pure ChEMBL ($\tau=5$) and similarly, in the validation split between ($\nu=0.0$) and ($\nu=1.0$), respectively.

Figure 1 illustrates the variations of average V-wF1 and V-PPPL versus the standardization noise in the training and validation splits. Here, increasing the percentages of ChemBL-standardized SMILES in each split increases the average value of V-PPPL for all variants of BERT. For instance, the V-PPPL for Tiny-BERT increases from 1.7715 ± 0.0587 to 3.6218 ± 0.2487 and 2.6416 ± 0.1838 when SMILES in the pure PubChem ($\tau=\nu=0$) dataset are completely replaced by their ChemBL-standardized counterparts in the training ($\tau=5, \nu=0$) or validation splits ($\tau=0, \nu=1.0$), respectively. In an extreme case where the entire training data is replaced with ChEMBL-standardized SMILES ($\tau=5, \nu=0$), Tiny-BERT shows signs of divergence which triggers the early stopping mechanism after a few epochs, in all three independent runs (see Supporting Information for more details). Therefore, the model’s ability to predict the masked tokens in the input sequences can be severely hampered by the standardization noise when the model is trained and validated on SMILES with mixed

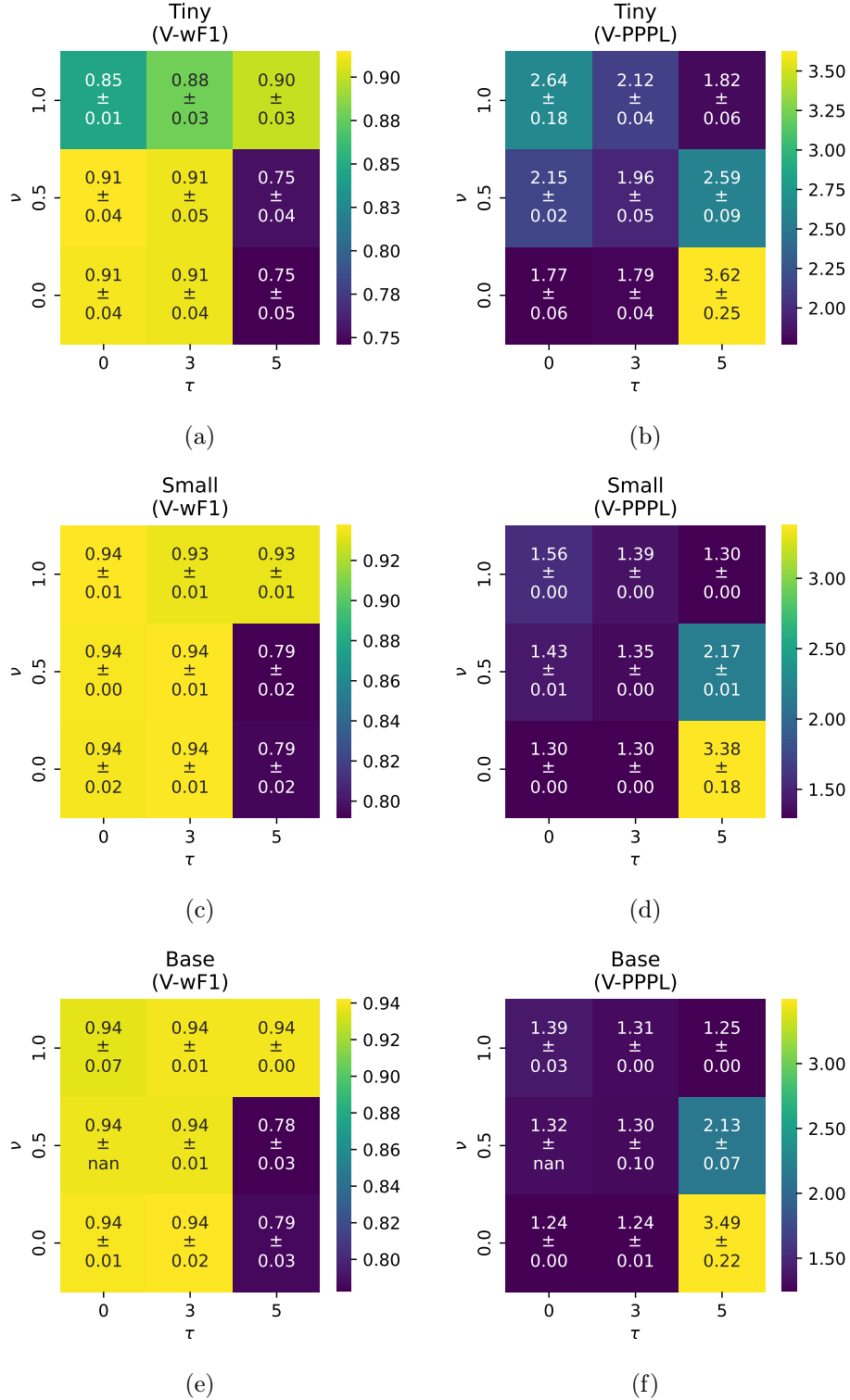


Figure 1: The effect of standardization noise on the pre-training validation weighted-F1 score (a,c,e) and pseudo-perplexity (b,d,f) of BERT for masked language modeling. Both metrics are averaged over three independent runs with different data sampling and model initialization seeds. τ and ν control the standardization noise in the pre-training and validation splits, respectively. The error bars are based on 95% confidence interval which are not defined (NaN) for samples of $N = 1$ runs, if the other two have diverged and removed from calculating the statistical summaries.

standardization protocols. This observation is consistent with the observed degradation in V-wF1 score as the SMILES standardization noise in the training and validation splits increases. Other performance metrics such as V-Loss and V-Acc show similar trends and are presented in Fig. 1 of the Extended Data.

Figure 1 also demonstrates that larger models become more resilient to the standardization noise, as evidenced by the V-wF1 and V-PPPL values, going from the top to bottom row. The impact of the standardization noise on the model performance can be minimized via taking the “path of least destruction” (the diagonal parts of the heatmaps in Fig. 1) where the standardization noise is gradually added to both training and validation splits, simultaneously. Here, we assume the SMILES, added to both splits, are generated by the same or similar data distributions.

The Effect of Tokenization on Pre-training

The tokenization process is a crucial step in the pre-training of LLMs for MPP tasks as it determines how the input sequences are processed by the models and what their vocabulary composition will be. In this study, we investigate the impact of WordPiece³⁷ and Byte Pair Encoding (BPE)³⁸ tokenization algorithms on the pre-training performance of BERT. Both algorithms start with a base vocabulary of individual characters and iteratively apply the learned merging rules to form new tokens until a pre-defined vocabulary size is reached. The main difference between the two algorithms is that the WordPiece algorithm uses a likelihood-based criterion to select the subword units for merging while BPE relies on a frequency-based criterion.^{37,38} Regardless of the selected tokenization method, the average metric values improve as the model size increases from Tiny-BERT, to Base-BERT. For instance, the magnitude of V-PPPL decreases from 1.5978 ± 0.0138 (1.5435 ± 0.0332) to 1.1450 ± 0.0052 (1.1233 ± 0.0125) using WordPiece (BPE) tokenizer— an improvement of 28% for WordPiece and 27% for BPE. As the sample size (*i.e.*, the number of experiments) for each model variant is small ($N \leq 3$), we refrain from making any judgments on the

statistical significance based on the estimated confidence interval (CI) and choose to proceed with WordPiece as our tokenizer, consistent with the original BERT model.¹² For further details on the tokenization experiments, see Table 2 in the Extended Data.

The Effect of Dataset and Model Sizes on Pre-training

In order to study the effect of dataset size on the pre-training performance, we create six dataset bins with the number of training samples in each bin following an exponential expression of the form

$$N_{\text{train}} = a \times 2^k + b, \quad (1)$$

where the bin indices, $k = 0, 1, 2, 3, 4$ and 5 , correspond to 2.5%, 5%, 10%, 20%, 40% and 80% of the data, respectively. Here, $a = 2,979,620$ fixes the size of the first bin and b is the correction factor, which ensures that the addition of the sixth bin ($k = 5$) will exactly cover 80% of the PubChem dataset. As such, $b = 4$ when $k = 5$ and zero otherwise.

Having a coherent standardization protocol in place, we expect the pre-training performance to improve as the dataset and model sizes increase.^{34,35} This is indeed the case as shown in Fig. 2. For all three variants of BERT, the average pre-training V-Loss decreases as the dataset size increases (Fig. 2a). For each bin index k , the magnitude of the average V-Loss also decreases as the model size increases from Tiny-BERT to Base-BERT. Similar trends are observed for V-PPPL (Fig. 2d) which suggest that larger models are more effective at learning the syntax and semantics of the language of chemistry via MLM pre-training.

It is important to note that both V-Loss and V-PPPL show a sudden change in the slope of their diagrams at around $k = 2$ which corresponds to training on 10% of the data (≈ 12 million samples). This change can be an indication of a critical threshold in dataset size, beyond which the performance improvements start to plateau. Furthermore, the performance gap is more pronounced at smaller dataset sizes, especially between Tiny- and Small-BERT variants, but it tends to diminish as the dataset size increases. This suggests

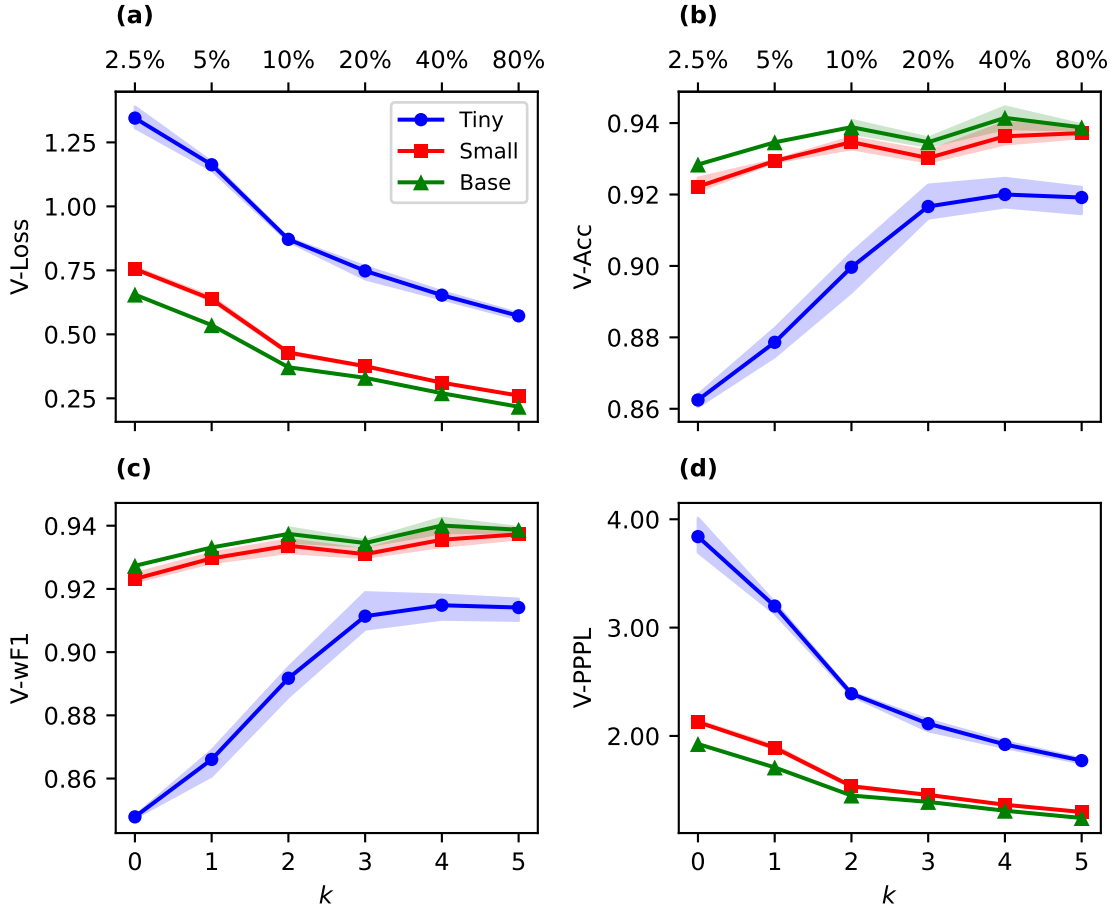


Figure 2: Variations of BERT’s pre-training performance metrics: (a) validation loss (V-Loss), (b) accuracy (V-Acc), (c) weighted-F1 score (V-wF1), and (d) pseudo-perplexity (V-PPPL) versus the dataset size bin index, k (the corresponding data percentages are shown on the top axes). Results pertinent to the Tiny-, Small- and Base-BERT are shown in blue circles, red squares and green triangles, respectively. Shaded bands are used to indicate the 95% confidence intervals across three independent runs with different model initialization and data sampling random seeds.

that larger models are more sample efficient and can achieve better performance with smaller samples of data compared to their smaller size counterparts, which is consistent with previous studies.^{34,35} Figure 2b and c illustrate the variations of V-Acc and V-wF1 with respect to the dataset size. The magnitude of both metrics increases as the dataset size increases, with the performance gap between the different model variants being more noticeable at smaller dataset sizes, especially between Tiny- and Small-BERT variants. However, the aforementioned performance gap diminishes as the dataset size increases. At around $k = 3$, corresponding to training on 20% of the data (~ 24 million samples), both V-Acc and V-wF1 for Tiny-BERT show a sudden change in the slope of their corresponding diagrams, after which the performance improvements starts to plateau. Notably, the magnitude of V-Acc and V-wF1 for both Small- and Base-BERT variants show a small dip at around $k = 3$ but continue to increase on average, as the dataset size increases.

Model and Dataset Size Effects on Fine-tuning

In this section, we use Biogen’s absorption, distribution, metabolism and excretion (ADME) public dataset to investigate the impact of pre-training dataset and model sizes on the fine-tuning performance of BERT for downstream MPP regression tasks.³⁹ The fine-tuning is performed using 3-fold cross-validation on the training split where 20% of data was set aside for testing and the remaining 80% was split into three folds, with two folds used for training and one fold used for validation within three iterations. A Bayesian hyperparameter search over 50 model architectures is performed on each fold using foundation models, which were trained on 2.5%, 20% and 80% (or $k=0, 3$, and 5) of the PubChem data. The best model from each search is selected based on the validation R^2 metric, following Ref. 39. For each k , the top performing cross-validated model is then refitted on the entire (training and validation) fine-tuning data and evaluated on a test set. The cross-validation outcomes for the human liver microsomal (HLM), human plasma protein binding (hPPB) and solubility endpoints are shown in Figs. 2–4 of Extended Data.

The average 3-fold cross-validation performance metrics for the HLM and hPPB endpoints indicate that the Pearson R and R^2 increase for all variants of BERT as the pre-training dataset size increases. The opposite trends are observed for the regression error metrics where the average mean absolute error (MAE) and root mean square error (RMSE) values decrease as the pre-training dataset size increases. These trends highlight the importance of pre-training dataset size for improving the fine-tuning performance of BERT on the downstream tasks. Furthermore, for each pre-training dataset size (bin index k), the performance improves as the model size increases from Tiny-BERT to Base-BERT. Note that the cross-validation results for the solubility endpoint are significantly impacted by the large standard deviations (≈ 0.68) and the strongly skewed nature of the distribution of the experimental data.³⁹ As such, providing a fair assessment of the cross-validation results for the solubility endpoint is challenging.

The testing performance results for BERT on the HLM, hPPB and solubility endpoints are presented in Figs. 3–5. The test Pearson R and R^2 values for all variants of BERT increase as the pre-training dataset size increases. The opposite trends are observed for the regression error metrics where the average MAE and RMSE values decrease as the pre-training dataset size increases. These trends further confirm the importance of pre-training dataset size for improving the fine-tuning performance of BERT on the downstream tasks and are consistent with the empirical scaling laws of LLMs.^{34,35} Here, caution should be exercised in making direct comparisons due to the differences in the model architecture and the training objectives.

We extend the fine-tuning results to all endpoints using BERT foundation models that are trained on 80% ($k=5$) of PubChem data. For comparison, we have also fine-tuned a set of classical ML models such as least absolute shrinkage and selection operator (LASSO), random forest (RF), support vector machine (SVM), extreme gradient boosting (XGB), and light gradient boosting machine (LGBM) on the same training and validation splits using the fine-tuning procedure mentioned above. The only caveat is that we used grid search

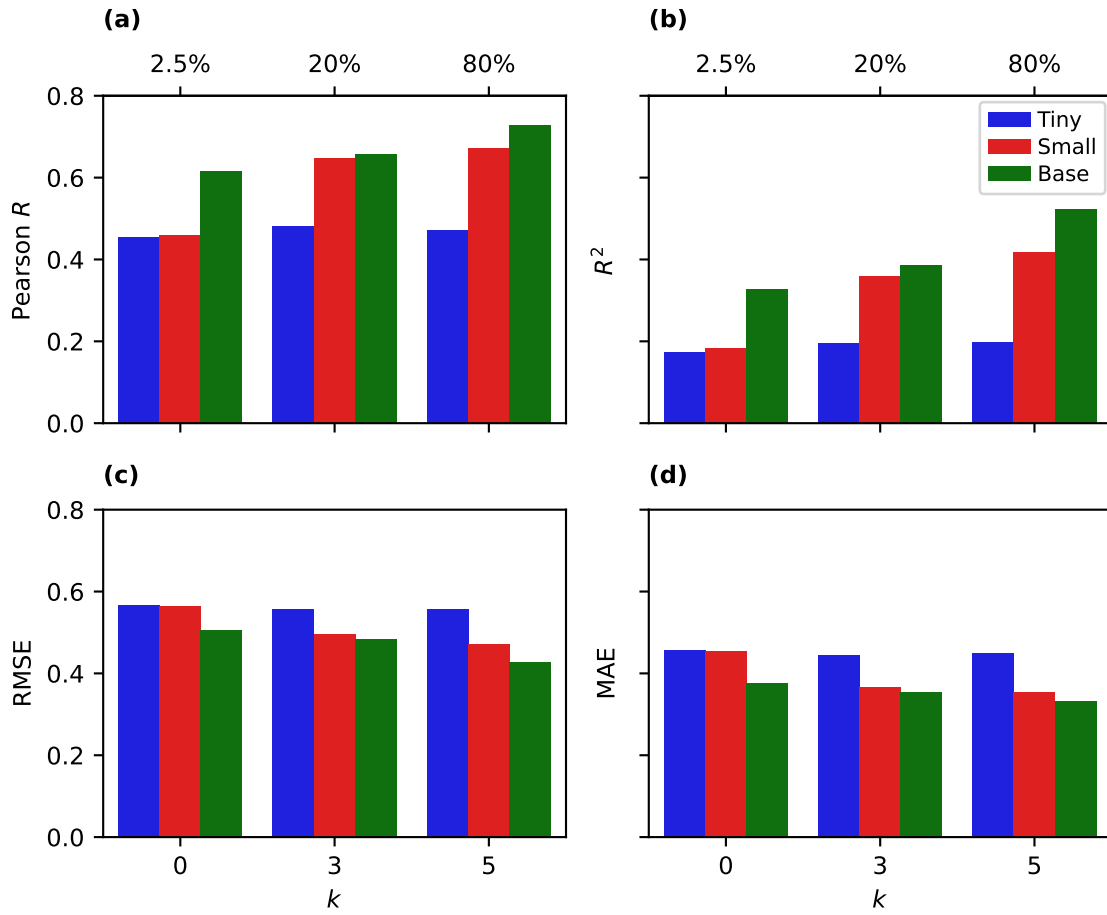


Figure 3: Variations of the fine-tuned BERT’s testing performance metrics, (a) Pearson R , (b) R^2 , (c) RMSE, (d) MAE, versus the pre-training dataset size bin index, k , for the HLM endpoint (the corresponding data percentages are shown on the top axes)

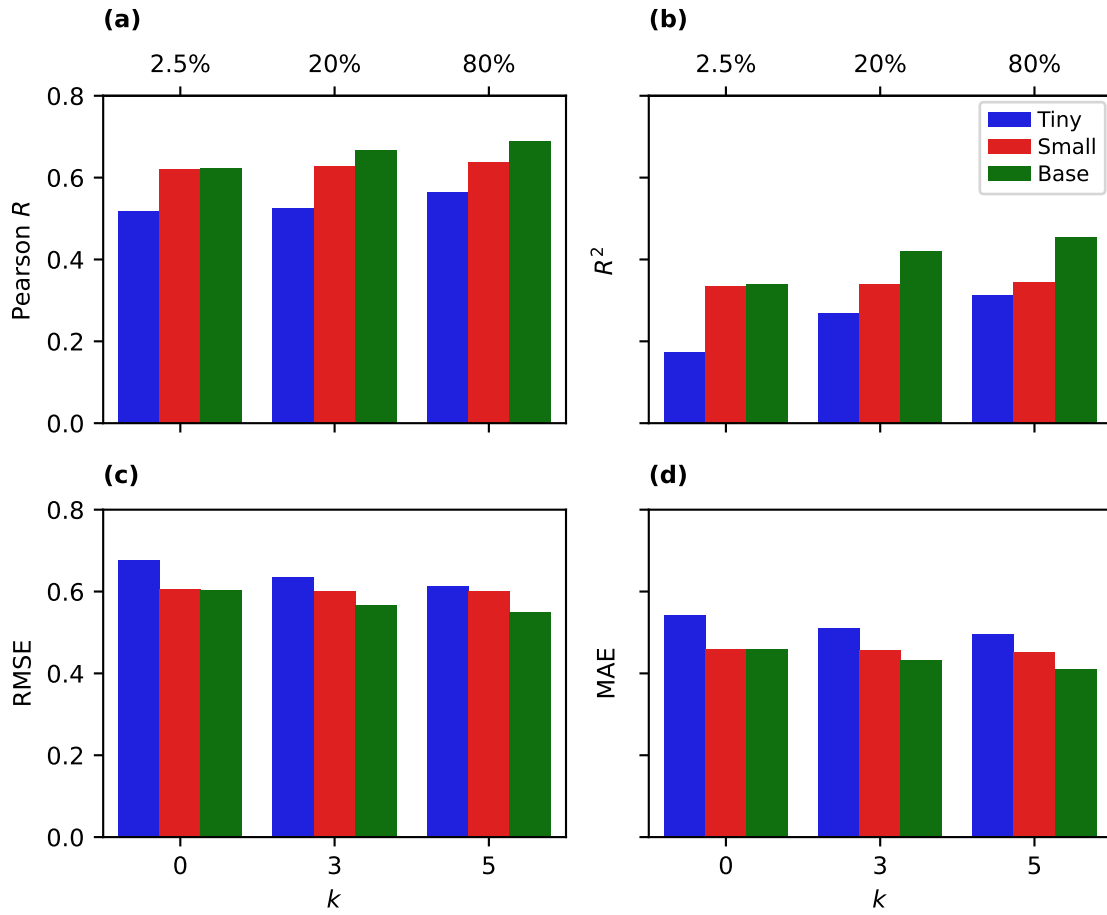


Figure 4: Variations of the fine-tuned BERT’s testing performance metrics, (a) Pearson R , (b) R^2 , (c) RMSE, (d) MAE, versus the pre-training dataset size bin index, k , for the hPPB endpoint (the corresponding data percentages are shown on the top axes)

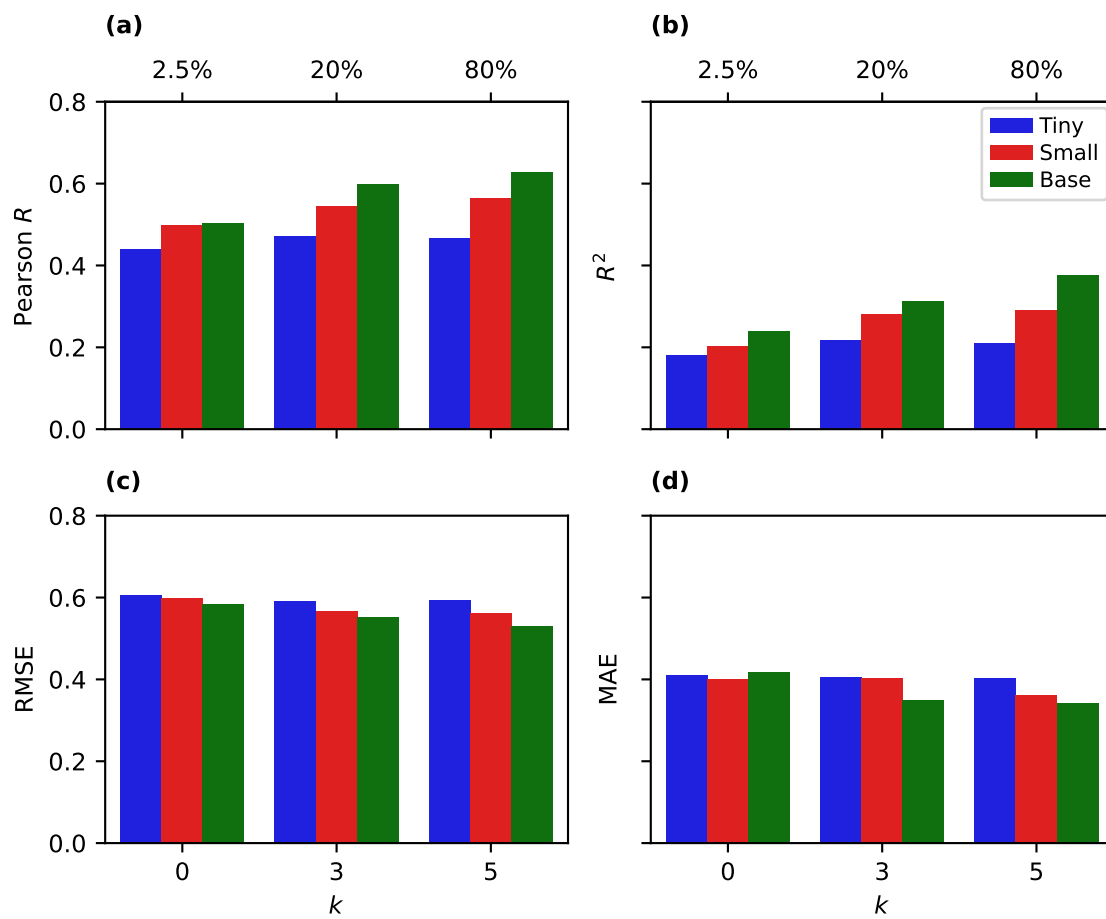


Figure 5: Variations of the fine-tuned BERT’s testing performance metrics, (a) Pearson R , (b) R^2 , (c) RMSE, (d) MAE, versus the pre-training dataset size bin index, k , for the solubility endpoint (the corresponding data percentages are shown on the top axes)

instead of Bayesian search for the hyperparameter optimization of the classical models to be consistent with the training process adopted in Ref. 39.

The fine-tuning results (Tables 4–9 of the Supporting Information) demonstrate that the testing performance of Base-BERT is superior or similar to those of the classical ML models for all six endpoints. The hPPB and rat plasma protein binding (rPPB) endpoints show testing performance results for Base-BERT that are competitive to those of classical ML models. Unfortunately, both endpoints have the smallest sample sizes (1808 and 885 data-points before preprocessing, respectively) of mixed sources (ChEMBL and Biogen) and have two of the largest standard deviations in their experimental values among all six endpoints (>0.6), which makes it challenging for the models to generalize well on even smaller test sets (20% of the total dataset size).³⁹

Discussion

Recent results,^{25,28,32,33} focusing on the pre-training and fine-tuning of LLMs on MPP downstream tasks, show trends that are inconsistent and contradictory. For example, Chen *et al.*³² pre-trained a variant of BERT on three combinations of SMILES from ChEMBL (<https://www.ebi.ac.uk/chembl>), PubChem (<https://pubchem.ncbi.nlm.nih.gov>) and ZINC (<https://zinc.docking.org>) databases. The three sets involve 1,941,410 compounds from ChEMBL, 103,395,400 compounds from ChEMBL and PubChem, and 775,007,514 compounds from ChEMBL, PubChem and ZINC. The resulting foundation models were subsequently fine-tuned on 10 downstream regression and classification MPP tasks from MoleculeNet.⁴⁰ Surprisingly, the model pre-trained on the smallest dataset outperformed the other models in 7 out of 10 tasks. Similar observations were documented in a recent review.³³

In the absence of well-established scaling laws for encoder-only models with a MLM objective, we resort to conducting hundreds of carefully controlled experiments to systematically investigate how factors such as dataset size, model size, tokenization, model architecture and

standardization can influence the performance of CLM for MPP.

Our results suggest that choosing different random seeds for model initialization and data sampling (Table 1) or choosing between WordPiece and BPE tokenization algorithms (Table 2 of Extended Data) have minor effects on the pre-training performance of BERT compared to the choice of model size and dataset size. Both observations are consistent with the scaling laws of auto-regressive LLMs.^{34,35}

Our experiments highlight the importance and overarching role of datasets, standardization protocols, and experimental settings in pre-training and fine-tuning performance of BERT for MPP tasks. We choose PubChem for pre-training our models as it is one of the largest publicly available general-purpose chemical databases with over 119 million unique compounds with their associated properties. PubChem offers a user-friendly interface for accessing, searching and downloading the data. Furthermore, PubChem provides a rigorous standardization pipeline⁴¹ which can mitigate potential data quality and consistency issues observed in non-standardized databases.

As a crucial step in data preprocessing, standardization transforms the SMILES representation of chemical structures into a consistent and unique form that is aligned with the intended domain-specific applications of the underlying databases. We hypothesize that studies^{25,28,32,33} which combine SMILES from various chemical databases to create bigger pre-training sets to improve the performance of their models on the downstream tasks, may have inadvertently introduced standardization noise by mixing different standardization protocols. We test this hypothesis by replacing various percentages of the PubChem SMILES in the training and validation splits with their corresponding ChEMBL-standardized counterparts and study its impact on the pre-training performance of BERT via V-loss, V-Acc, V-wF1 and V-PPPL metrics (see Fig. 1, Extended Data and Supporting Information). Figure 1 demonstrates that the standardization noise can severely degrade the pre-training performance of BERT. Furthermore, larger models tend to be more resilient to the standardization noise, especially if the noise, added to both training and validation splits, follows the “path of least

destruction” (the diagonal parts of the heatmaps in Fig. 1) while its distribution in both splits does not drastically change.

The choice of benchmark dataset is another important factor. Unfortunately, the majority of the studies involving CLMs have adopted the MoleculeNet dataset for fine-tuning and evaluation purposes. MoleculeNet is a collection of 17 datasets across four domains of quantum chemistry, physical chemistry, biophysics, and physiology. This dataset includes both regression and classification objectives and is designed for benchmarking ML models for MPP.⁴⁰ Despite its popularity, MoleculeNet suffers from major issues such as invalid structures, inconsistent chemical representations, ambiguous stereochemistry, duplicate entries with conflicting property values *etc.*⁴² Such issues are not specific to MoleculeNet and can be found in other popular datasets such as Therapeutics Data Commons (TDC), accessible from <https://tdcommons.ai>.

Here, we use the curated Biogen ADME dataset for fine-tuning and evaluating our models on six ADME regression endpoints: HLM, rat liver microsomal (RLM), hPPB, rPPB, MDR1-MDCK efflux ratio (MDR1-MDCK ER) and solubility.³⁹ We standardize all SMILES using PubChem’s standardization protocol and tokenize them using the WordPiece tokenizer. Our 3-fold cross-validation hyperparameter search results indicate that the testing performance of BERT on the studied ADME tasks (Figs. 3–5) consistently improves as the pre-training dataset and model sizes increase. These trends are consistent with the scaling laws of autoregressive LLMs,^{34,35} although not directly transferrable to encoder-only models with MLM objectives.

Additional cross-validation and testing results with BERT foundation models, pre-trained on all 80% ($k=5$) of the PubChem data, demonstrate that the testing performance of Base-BERT is superior or similar to those of the classical ML models for all ADME endpoints. Judging by the differences between the average error metrics of the best performing models, the choice of pre-training and fine-tuning a CLM for downstream MPP tasks becomes an economical one. That is, depending on the task at hand and the available resources, one

should weigh the benefits of using a CLM against the costs and complexities associated with pre-training and fine-tuning it. While classical ML models can be trained and fine-tuned much faster and with less computational resources, CLMs often require significant computational resources and time for pre-training. Meanwhile, foundation CLMs possess a general understanding of the chemical language and can be fine-tuned on a wide range of downstream tasks with relatively small labeled datasets and affordable training times, often with a performance boost compared to their classical counterparts.

In summary, we have provided numerical evidence from hundreds of experiments which favor the potential existence of a scaling law for encoder-only CLMs with MLM objectives. Our results highlight the importance of (pre-training, fine-tuning and benchmarking) datasets, standardization protocols and experimental settings. We demonstrate that larger high-quality pre-training datasets processed by well-defined and coherent standardization protocols lead to better pre-training and fine-tuning performance on downstream MPP tasks. We have also delineated that larger models are more sample efficient, noise resilient and performant in both pre-training and fine-tuning settings. While our analyses are based on qualitative trends observed within small statistical samples of experiments, the extraction of exact quantitative relations requires a more comprehensive set of experiments which will be the subject of our ongoing and future studies.

Methods

Statistical Analysis of the Results

Throughout this work, in order to account for the data variability and to provide an estimate for a range of plausible values for the true population metrics, we often accompany our measurements of the property x of a sample of size N , with a 95% CI, which is defined as

$$\text{CI}(x) = \bar{x} \pm \left(\frac{s_N}{\sqrt{N}} \right) t_{95\%, N-1}. \quad (2)$$

Here, $t_{95\%,N-1}$ denotes the critical value from the Student’s t -distribution with $N - 1$ degrees of freedom at 95% confidence level. Also, \bar{x} and s_N are the sample mean and the standard deviation of the quantity x , respectively, which can be expressed as

$$\bar{x} = \frac{1}{N} \sum_{i=1}^N x_i, \quad \text{and} \quad s_N = \sqrt{\frac{1}{N-1} \sum_{i=1}^N (x_i - \bar{x})^2}, \quad (3)$$

where x_i is the i -th input data or measurement outcome.

Since pre-training LLMs is very expensive (see Supporting Information for more details) our sample sizes are often small where the number of experiments $N = 3$ or 5 . As such, in interpreting the error bars and comparing the results of various experiments, it is imperative to highlight the adoption of a conventional value for $t_{95\%,N-1}$ which is often set to 1.96. While this value maybe appropriate for large sample sizes, care must be taken in calculating the error bars for very small sample sizes. In such cases, the critical value $t_{95\%,N-1}$ can be much larger than 1.96, which can lead to a significant overestimation of the error bars and misinterpretation of the results. In order to mitigate the impact of small sample sizes on the error bars, we use NIST’s “Critical Values of the Student’s t Distribution” table from Ref. 36 to determine the appropriate $t_{95\%,N-1}$ for each sample size. Here, we do not provide the Cohen’s d or Hedges’ g for calculating the effect size and comparing the results of different experiments.

Performance and Error Metrics

This section summarizes all metrics that are adopted for evaluating the performance of BERT models during pre-training and fine-tuning. Let $\mathbf{x}^i = (x_1^i, \dots, x_T^i)$ be the i th sequence of tokens such as word, wordpieces *etc.* Each token, x_t^i , can categorically assume one of the W entries from a vocabulary $\mathbf{v} = \{v_1, \dots, v_W\}$ which also includes special entries such as [UNK], reserved to represent out-of-vocabulary tokens. We also create a masked variant of the original sequence, $\mathbf{x}_{\setminus t}^i$, by randomly replacing a portion (*e.g.*, 15%) of the tokens in

the sequence with a special token [MASK]. For example, masking a token at position index t , belonging to $\mathcal{M}_i \subseteq \{1, \dots, T_i\}$, yields $\mathbf{x}_{\setminus t}^i = (x_1^i, \dots, x_{t-1}^i, [\text{MASK}], x_{t+1}^i, \dots, x_{T_i}^i)$. The objective of the MLM is to reconstruct the original sequence from its corrupted version by minimizing the negative pseudo log-likelihood (cross-entropy) loss function defined as

$$\min_{\theta} \mathcal{L}(\theta; \mathcal{D}) = - \frac{\sum_{i=1}^{|\mathcal{D}|} \sum_{t=1}^{T_i} \mathbb{I}_{\mathcal{M}_i}(t) \log p_{\theta}(x_t^i | \mathbf{x}_{\setminus t}^i)}{\sum_{i=1}^{|\mathcal{D}|} |\mathcal{M}_i|}. \quad (4)$$

Here, the denominator is the total number of masked tokens in the dataset and the conditional probability $p_{\theta}(x_t^i | \mathbf{x}_{\setminus t}^i)$ is the probability of observing the original token x_t^i in the i th sequence given its corrupted version $\mathbf{x}_{\setminus t}^i$ and model parameters θ . The indicator function, $\mathbb{I}_{\mathcal{M}_i}(t)$, is equal to 1 if $t \in \mathcal{M}_i$ and zero otherwise which means, only masked tokens will directly contribute to the MLM loss. The semi-colon in $\mathcal{L}(\theta; \mathcal{D})$ highlights the difference between model parameters, θ , treated as variables, and the training data, \mathcal{D} considered as constants. Note that the pre-training process is an example of self-supervised learning because the original tokens in each sequence, taken as labels, are the generators of their masked counterparts in the dataset; *i.e.*, $\mathcal{D} = \{(\mathbf{x}_{\setminus t}^i, \mathbf{x}^i)\}_{i=1}^{|\mathcal{D}|}$.

Using Eq. 4, we can express the model’s pseudo-perplexity (PPPL) on the pre-training dataset as⁴³

$$\text{PPPL}(\theta; \mathcal{D}) = \exp \left(- \frac{1}{\sum_{i=1}^{|\mathcal{D}|} |\mathcal{M}_i|} \sum_{i=1}^{|\mathcal{D}|} \sum_{t=1}^{T_i} \mathbb{I}_{\mathcal{M}_i}(t) \log p(x_t^i | \mathbf{x}_{\setminus t}^i) \right), \quad (5)$$

Similar to the BART paper,⁴⁴ we will also consider the accuracy and weighted-F1 score in the context of MLM. Assuming each entry in the vocabulary is a class, the accuracy can then be converted into a series of binary classification tasks in a one-versus-rest fashion and be expressed as

$$\text{Acc}(\theta; \mathcal{D}) = \frac{1}{\sum_{i=1}^{|\mathcal{D}|} |\mathcal{M}_i|} \sum_{i=1}^{|\mathcal{D}|} \sum_{t=1}^{T_i} \mathbb{I}_{\mathcal{M}_i}(t) [\mathbb{I}(\hat{x}_t^i = v_w, x_t^i = v_w) + \mathbb{I}(\hat{x}_t^i \neq v_w, x_t^i \neq v_w)], \quad (6)$$

where the unmasked reference token, $v_w \in \mathbf{v}$, denotes the positive class and $\hat{x}_t^i = \operatorname{argmax}_{x_t^i \in \mathbf{v}} p_\theta(x_t^i | \mathbf{x}_{\setminus t}^i)$, is the action of choosing the most probable token, predicted by the model, from the vocabulary. In Eq. 6, we have also used the abbreviation

$$\mathbb{I}(\hat{x}_t^i = v_w, x_t^i = v_w) = \mathbb{I}(\hat{x}_t^i = v_w) \mathbb{I}(x_t^i = v_w). \quad (7)$$

In order to account for token frequency imbalance in the vocabulary, we report weighted-F1 score, which is defined as

$$\text{wF1}(\theta; \mathcal{D}) = \frac{\sum_{w=1}^W N_{v_w} \times \text{F1}_{v_w}}{\sum_{w=1}^W N_{v_w}}. \quad (8)$$

where,

$$N_{v_w} = \sum_{i=1}^{|\mathcal{D}|} \sum_{t=1}^{T_i} \mathbb{I}_{\mathcal{M}_i}(t) \mathbb{I}(x_t^i = v_w), \quad (9)$$

is the support or frequency of the token v_w at the masked positions within all sequences in the entire dataset and F1_{v_w} is the F1 score calculated for the token v_w as the positive class. The F1 score itself is expressed as the harmonic mean of precision and recall for each token (class) as

$$\text{F1}(\theta; \mathcal{D}) = \frac{2 \times \text{Precision} \times \text{Recall}}{\text{Precision} + \text{Recall}}, \quad (10)$$

where

$$\text{Precision} = \frac{TP}{TP + FP}, \quad (11)$$

$$\text{Recall} = \frac{TP}{TP + FN}. \quad (12)$$

In the context of MLM, the true positive (TP) and true negative (TN) are the number of masked tokens that are correctly predicted, and the false positive (FP) and false negative

(FN) are the number of masked tokens that are incorrectly predicted. More specifically,

$$TP = \sum_{i=1}^{|\mathcal{D}|} \sum_{t=1}^{T_i} \mathbb{I}_{\mathcal{M}_i}(t) \mathbb{I}(\hat{x}_t^i = v_w, x_t^i = v_w), \quad (13)$$

$$FP = \sum_{i=1}^{|\mathcal{D}|} \sum_{t=1}^{T_i} \mathbb{I}_{\mathcal{M}_i}(t) \mathbb{I}(\hat{x}_t^i = v_w, x_t^i \neq v_w), \quad (14)$$

$$TN = \sum_{i=1}^{|\mathcal{D}|} \sum_{t=1}^{T_i} \mathbb{I}_{\mathcal{M}_i}(t) \mathbb{I}(\hat{x}_t^i \neq v_w, x_t^i \neq v_w), \quad (15)$$

$$FN = \sum_{i=1}^{|\mathcal{D}|} \sum_{t=1}^{T_i} \mathbb{I}_{\mathcal{M}_i}(t) \mathbb{I}(\hat{x}_t^i \neq v_w, x_t^i = v_w). \quad (16)$$

Datasets

All variants of BERT in this study are pre-trained the PubChem dataset (version 4/18/2025), which is comprised of 119,184,806 unique chemical compounds represented by standardized canonical isomeric SMILES. Before pre-training, the data was randomly split into training and validation sets with 95,347,844 data points ($\sim 80\%$ of the data) and 23,836,962 data points ($\sim 20\%$ of the data), respectively.

We use Biogen’s ADME database³⁹ for fine-tuning and evaluation of our models for regression tasks. The dataset contains groups of 885 to 3087 compounds with their corresponding experimental measurement values for six *in vitro* ADME endpoints: HLM stability reported as intrinsic clearance (CL_{int}) in mL min⁻¹ kg⁻¹, MDR1-MDCK efflux ratio (MDR1-MDCK ER), solubility at pH 6.8 (μg mL⁻¹), RLM stability reported as CL_{int} in mL min⁻¹ kg⁻¹, hPPB in percent unbound and rPPB in percent unbound. The procedures for all experimental measurements are described in Ref. 39.

Standardization

We use two different standardization pipelines for data-preprocessing: (i) PubChem’s standardization pipeline which is based on OpenEye’s OEChem toolkit (<https://docs.eyesopen.com>).

com/toolkits/python/oechemtk) and (ii) ChEMBL’s standardization pipeline which is based on RDKit (<https://www.rdkit.org>). The details of both standardization workflows are summarized in the Supporting Information and further technical details can be found in Refs. 41 and 45.

Tokenization

The tokenization step happens before the pre-processed and standardized SMILES strings are fed into the model. Tokenization refers to the process of breaking down the input text into smaller units called tokens, which can be words, subwords, or characters. Some of the most popular tokenization methods in NLP are WordPiece,³⁷ BPE,³⁸ and Unigram (SentencePiece).⁴⁶ In chemistry, some groups have considered using regular expressions to tokenize the SMILES strings into meaningful subunits⁴⁷ or use them within BPE tokenization algorithm.⁴⁸

In this study, we use Hugging Face’s `tokenizers` and `transformers` libraries to implement and train the WordPiece and BPE tokenizers on the PubChem standardized canonical isomeric SMILES from scratch. We then compare the impact of the two tokenization methods on the pre-training. In order to ensure a fair comparison between the two tokenizers, we restrict the vocabulary size to 30522 tokens and limit the maximum sequence length to 512 tokens for both tokenizers. A minimum frequency threshold of 2 is used during training to filter out rare tokens. All experiments are conducted for a maximum of 5 epochs. Each experiment is repeated three times with different random seeds for model initialization and data sampling. The performance metrics for the tokenizers are reported in Table 2 of the Extended Data section.

Pre-training

In order to allow foundation LLMs learn the underlying structure, patterns and semantics of the chemical language, we pre-train BERT on the PubChem’s standardized canonical

isomeric SMILES using the MLM objective. In MLM, a certain percentage of the input tokens (in this work, 15%) are randomly masked and the model is trained to predict the original tokens based on the context provided by the unmasked tokens. Following RoBERTa’s objective design,⁴⁹ we use dynamic masking where the masking pattern is changed for every batch on-the-fly during training. This means that the model is exposed to different masked tokens in each epoch, which can help improve the model’s ability to learn from the entire input data and prevent overfitting. We do not include the next sentence prediction (NSP) objective in our pre-training because it is not pertinent to the downstream tasks considered in this work. Furthermore, several works have questioned its necessity for natural language understanding.^{49,50} The pre-training is performed using the AdamW optimizer with $\beta_1 = 0.9$, $\beta_2 = 0.999$, and $\epsilon = 10^{-8}$, a learning rate of 10^{-4} , a weight decay of 0.01 and an effective global batch size of 1024 (see the Supporting Information for more details).

Finetuning with Hyperparameter Search and Cross-validation

All variants of pre-trained BERT models in this study are fine-tuned on the Biogen ADME dataset for regression tasks, which involves predicting the experimental values for six *in vitro* ADME endpoints: HLM, RLM, hPPB, rPPB, MDR1-MDCK ER and solubility.³⁹ All SMILES are standardized using PubChem’s standardization protocol and tokenized using the WordPiece tokenizer. Fine-tuning is performed using 3-fold cross-validation where the dataset is split into three folds, with two folds used for training and one fold used for validation in each of the three iterations. A Bayesian hyperparameter search over 50 model architectures is performed on each fold using various foundation models, pre-trained on different dataset sizes. Each model was trained for 100 epochs with early stopping based on the validation loss metric with 5 epochs of patience. The best model from each search is selected based on the validation R^2 metric, following Ref. 39. The top performing cross-validated model is then refitted on the entire (training and validation) data for a maximum of 20 epochs and evaluated on a held-out test set which was not used during the cross-validated

hyperparameter search. We compare the performance of our chemical LLMs with some of the best performing models from Ref. 39 which include a variety of ML models such as LASSO, RF, SVM, XGB, and LGBM. All steps of the cross-validated hyperparameter search and fine-tuning are performed for these models on the same training data folds as those used for our LLMs. Nonetheless, the hyperparameter search for these models is performed using the grid search method on a pre-defined set of hyperparameters taken from Ref. 39.

Data Availability

The machine-learning ready version of the PubChem (version 04/18/2025) dataset used for pre-training the BERT models in this study is available at <https://huggingface.co/datasets/molssiai-hub/pubchem-04-18-2025>. The original SDF files for PubChem Compounds are accessible from <https://ftp.ncbi.nlm.nih.gov/pubchem/Compound>. The Biogen ADME dataset, used for fine-tuning and evaluation of the BERT models, is provided in a public repository at <https://github.com/molecularinformatics/Computational-ADME> or <https://polarishub.io/datasets/biogen/adme-fang-v1>.

Code Availability

All scripts necessary for reproducing the results of this work including figures, tables, data split indices, data preprocessing, standardization, tokenization, pre-training and fine-tuning the BERT models are provided in <https://github.com/molssi-ai/bertology>. The ChEMBL standardization module can be accessed from https://github.com/chembl/ChEMBL_Structure_Pipeline. All training and fine-tuning artifacts, including the pre-trained BERT models and the fine-tuned models for the six ADME endpoints, trainer, optimizer, random-number generators as well as all monitoring logs for W&B, Tensorboard and MLFlow can be downloaded from the MolSSI’s Zenodo Community page (<https://zenodo.org/communities/molssi>).

Acknowledgement

The present work is funded by the National Science Foundation grant CHE-2136142. PS and MM acknowledge the Advanced Research Computing (<https://arc.vt.edu>) at Virginia Tech for providing computational resources and technical support that have contributed to the results reported in this manuscript. MM thanks OpenEye Scientific (Cādence Molecular Sciences) for providing a free academic license for their cheminformatics and modelling toolkits. MM is grateful to NVIDIA for providing two NVIDIA A100 GPUs via the NVIDIA Academic Hardware Grant Program which made the tasks of prototype design and testing a breeze throughout the course of this work.

References

- (1) David, L.; Thakkar, A.; Mercado, R.; Engkvist, O. Molecular representations in AI-driven drug discovery: a review and practical guide. *Journal of Cheminformatics* 2020 *12:1* **2020**, *12*, 56.
- (2) Deng, J.; Yang, Z.; Wang, H.; Ojima, I.; Samaras, D.; Wang, F. A systematic study of key elements underlying molecular property prediction. *Nature Communications* 2023 *14:1* **2023**, *14*, 6395.
- (3) Wigh, D. S.; Goodman, J. M.; Lapkin, A. A. A review of molecular representation in the age of machine learning. *Wiley Interdisciplinary Reviews: Computational Molecular Science* **2022**, *12*, e1603.
- (4) Musil, F.; Grisafi, A.; Bartók, A. P.; Ortner, C.; Csányi, G.; Ceriotti, M. Physics-Inspired Structural Representations for Molecules and Materials. *Chemical Reviews* **2021**, *121*, 9759–9815.
- (5) Wouters, O. J.; McKee, M.; Luyten, J. Estimated Research and Development Invest-

- ment Needed to Bring a New Medicine to Market, 2009-2018. *JAMA* **2020**, *323*, 844–853.
- (6) Editorial For chemists, the AI revolution has yet to happen. *Nature* **2023**, *617*, 438.
- (7) Kolmar, S. S.; Grulke, C. M. The effect of noise on the predictive limit of QSAR models. *Journal of Cheminformatics* **2021**, *13*, 92.
- (8) Pang, C.; Tong, H. H. Y.; Wei, L. Advanced deep learning methods for molecular property prediction. *Quantitative Biology* **2023**, *11*, 395–404.
- (9) Vaswani, A.; Shazeer, N.; Parmar, N.; Uszkoreit, J.; Jones, L.; Gomez, A. N.; Łukasz Kaiser; Polosukhin, I. Attention Is All You Need. *Advances in Neural Information Processing Systems* **2017**, *2017-December*, 5998–6009.
- (10) Weininger, D. SMILES, a Chemical Language and Information System: 1: Introduction to Methodology and Encoding Rules. *Journal of Chemical Information and Computer Sciences* **1988**, *28*, 31–36.
- (11) Bahdanau, D.; Cho, K.; Bengio, Y. Neural Machine Translation by Jointly Learning to Align and Translate. *3rd International Conference on Learning Representations, ICLR 2015 - Conference Track Proceedings* **2014**,
- (12) Devlin, J.; Chang, M. W.; Lee, K.; Toutanova, K. BERT: Pre-training of Deep Bidirectional Transformers for Language Understanding. *NAACL HLT 2019 - 2019 Conference of the North American Chapter of the Association for Computational Linguistics: Human Language Technologies - Proceedings of the Conference* **2019**, *1*, 4171–4186.
- (13) Hinton, G.; Vinyals, O.; Dean, J. Distilling the Knowledge in a Neural Network. **2015**, Preprint at <https://arxiv.org/abs/1503.02531v1>.
- (14) Han, S.; Mao, H.; Dally, W. J. Deep Compression: Compressing Deep Neural Networks

- with Pruning, Trained Quantization and Huffman Coding. *4th International Conference on Learning Representations, ICLR 2016 - Conference Track Proceedings* **2016**,
- (15) Li, Z.; Wallace, E.; Shen, S.; Lin, K.; Keutzer, K.; Klein, D.; Gonzalez, J. E. Train Large, Then Compress: Rethinking Model Size for Efficient Training and Inference of Transformers. *37th International Conference on Machine Learning, ICML 2020*, 119, 5958–5968.
- (16) Wang, S.; Guo, Y.; Wang, Y.; Sun, H.; Huang, J. SMILES-BERT: Large Scale Un-supervised Pre-Training for Molecular Property Prediction. Proceedings of the 10th ACM International Conference on Bioinformatics, Computational Biology and Health Informatics. New York, NY, USA, 2019; pp 429–436.
- (17) Honda, S.; Shi, S.; Ueda, H. R. SMILES Transformer: Pre-trained Molecular Fingerprint for Low Data Drug Discovery. **2019**, Preprint at <https://arxiv.org/abs/1911.04738v1>.
- (18) Fabian, B.; Edlich, T.; Gaspar, H.; Segler, M. H. S.; Meyers, J.; Fiscato, M.; Ahmed, M. Molecular representation learning with language models and domain-relevant auxiliary tasks. *arXiv* **2020**, Preprint at <https://arxiv.org/abs/2011.13230v1>.
- (19) Maziarka, Ł.; Danel, T.; Mucha, S.; Rataj, K.; Tabor, J.; Jastrzębski, S. Molecule Attention Transformer. *arXiv* **2020**, Preprint at <https://arxiv.org/abs/2002.08264v1>.
- (20) Karpov, P.; Godin, G.; Tetko, I. V. Transformer-CNN: Swiss knife for QSAR modeling and interpretation. *Journal of Cheminformatics* **2020**, 12, 17.
- (21) Li, J.; Jiang, X. Mol-BERT: An Effective Molecular Representation with BERT for Molecular Property Prediction. *Wireless Communications and Mobile Computing* **2021**, 2021, 7181815.

- (22) Xue, D.; Zhang, H.; Chen, X.; Xiao, D.; Gong, Y.; Chuai, G.; Sun, Y.; Tian, H.; Wu, H.; Li, Y.; Liu, Q. X-MOL: large-scale pre-training for molecular understanding and diverse molecular analysis. *Science Bulletin* **2022**, *67*, 899–902.
- (23) Wu, Z.; Jiang, D.; Wang, J.; Zhang, X.; Du, H.; Pan, L.; Hsieh, C. Y.; Cao, D.; Hou, T. Knowledge-based BERT: a method to extract molecular features like computational chemists. *Briefings in Bioinformatics* **2022**, *23*, bbac131.
- (24) Chithrananda, S.; Grand, G.; Ramsundar, B. ChemBERTa: Large-Scale Self-Supervised Pretraining for Molecular Property Prediction. **2020**, Preprint at <https://arxiv.org/abs/2010.09885v2>.
- (25) Ahmad, W.; Simon, E.; Chithrananda, S.; Grand, G.; Ramsundar, B. ChemBERTa-2: Towards Chemical Foundation Models. *arXiv* **2022**, Preprint at <https://arxiv.org/abs/2209.01712v1>.
- (26) Irwin, R.; Dimitriadis, S.; He, J.; Bjerrum, E. J. Chemformer: a pre-trained transformer for computational chemistry. *Machine Learning: Science and Technology* **2022**, *3*, 015022.
- (27) Wen, N.; Liu, G.; Zhang, J.; Zhang, R.; Fu, Y.; Han, X. A fingerprints based molecular property prediction method using the BERT model. *Journal of Cheminformatics* **2022**, *14*, 71.
- (28) Ross, J.; Belgodere, B.; Chenthamarakshan, V.; Padhi, I.; Mroueh, Y.; Das, P. Large-scale chemical language representations capture molecular structure and properties. *Nature Machine Intelligence* **2022**, *4*, 1256–1264.
- (29) Soares, E.; Brazil, E. V.; Aquino Gutierrez, K. F.; Cerqueira, R.; Sanders, D.; Schmidt, K.; Zubarev, D. Beyond Chemical Language: A Multimodal Approach to Enhance Molecular Property Prediction. *arXiv* **2023**, Preprint at <https://arxiv.org/abs/2306.14919v1>.

- (30) Zhang, J.; Du, W.; Yang, X.; Wu, D.; Li, J.; Wang, K.; Wang, Y. SMG-BERT: integrating stereoscopic information and chemical representation for molecular property prediction. *Frontiers in Molecular Biosciences* **2023**, *10*, 1216765.
- (31) Wu, F.; Radev, D.; Li, S. Z. Molformer: Motif-based Transformer on 3D Heterogeneous Molecular Graphs. *Proceedings of the 37th AAAI Conference on Artificial Intelligence, AAAI 2023* **2021**, *37*, 5312–5320.
- (32) Chen, D.; Zheng, J.; Wei, G. W.; Pan, F. Extracting Predictive Representations from Hundreds of Millions of Molecules. *Journal of Physical Chemistry Letters* **2021**, *12*, 10793–10801.
- (33) Sultan, A.; Sieg, J.; Mathea, M.; Volkamer, A. Transformers for Molecular Property Prediction: Lessons Learned from the Past Five Years. *Journal of Chemical Information and Modeling* **2024**, *64*, 6259–6280.
- (34) Kaplan, J.; McCandlish, S.; OpenAI, T. H.; OpenAI, T. B. B.; OpenAI, B. C.; OpenAI, R. C.; OpenAI, S. G.; OpenAI, A. R.; OpenAI, J. W.; OpenAI, D. A. Scaling Laws for Neural Language Models. **2020**, Preprint at <https://arxiv.org/abs/2001.08361v1>.
- (35) Hoffmann, J.; Borgeaud, S.; Mensch, A.; Buchatskaya, E.; Cai, T.; Rutherford, E.; de Las Casas, D.; Hendricks, L. A.; Welbl, J.; Clark, A.; Hennigan, T.; Noland, E.; Millican, K.; van den Driessche, G.; Damoc, B.; Guy, A.; Osindero, S.; Simonyan, K.; Elsen, E.; Vinyals, O.; Rae, J. W.; Sifre, L. Training Compute-Optimal Large Language Models. *Advances in Neural Information Processing Systems* **2022**, *35*.
- (36) NIST NIST/SEMATECH e-Handbook of Statistical Methods. 2012; <https://doi.org/10.18434/M32189>, Last Accessed: 03-02-2026.
- (37) Wu, Y.; Schuster, M.; Chen, Z.; Le, Q. V.; Norouzi, M.; Macherey, W.; Krikun, M.; Cao, Y.; Gao, Q.; Macherey, K.; Klingner, J.; Shah, A.; Johnson, M.; Liu, X.; Łukasz

- Kaiser; Gouws, S.; Kato, Y.; Kudo, T.; Kazawa, H.; Stevens, K.; Kurian, G.; Patil, N.; Wang, W.; Young, C.; Smith, J.; Riesa, J.; Rudnick, A.; Vinyals, O.; Corrado, G.; Hughes, M.; Dean, J. Google’s Neural Machine Translation System: Bridging the Gap between Human and Machine Translation. **2016**, Preprint at <https://arxiv.org/abs/1609.08144v2>.
- (38) Sennrich, R.; Haddow, B.; Birch, A. Neural Machine Translation of Rare Words with Subword Units. *54th Annual Meeting of the Association for Computational Linguistics, ACL 2016 - Long Papers* **2016**, *3*, 1715–1725.
- (39) Fang, C.; Wang, Y.; Grater, R.; Kapadnis, S.; Black, C.; Trapa, P.; Sciabola, S. Prospective Validation of Machine Learning Algorithms for Absorption, Distribution, Metabolism, and Excretion Prediction: An Industrial Perspective. *Journal of Chemical Information and Modeling* **2023**, *63*, 3263–3274.
- (40) Wu, Z.; Ramsundar, B.; Feinberg, E. N.; Gomes, J.; Geniesse, C.; Pappu, A. S.; Leswing, K.; Pande, V. MoleculeNet: a benchmark for molecular machine learning. *Chemical Science* **2018**, *9*, 513–530.
- (41) Hähnke, V. D.; Kim, S.; Bolton, E. E. PubChem chemical structure standardization. *Journal of Cheminformatics* **2018**, *10*, 36.
- (42) Walters, W. P. We Need Better Benchmarks for Machine Learning in Drug Discovery. 2023; <https://practicalcheminformatics.blogspot.com/2023/08/we-need-better-benchmarks-for-machine.html>, Last Accessed: 2026-02-23.
- (43) Salazar, J.; Liang, D.; Nguyen, T. Q.; Kirchoff, K. Masked Language Model Scoring. Proceedings of the 58th Annual Meeting of the Association for Computational Linguistics. 2020; pp 2699–2712.
- (44) Lewis, M.; Liu, Y.; Goyal, N.; Ghazvininejad, M.; Mohamed, A.; Levy, O.; Stoyanov, V.; Zettlemoyer, L. BART: Denoising Sequence-to-Sequence Pre-training for Natural Lan-

- guage Generation, Translation, and Comprehension. *Proceedings of the Annual Meeting of the Association for Computational Linguistics* **2019**, 7871–7880.
- (45) Bento, A. P.; Hersey, A.; Félix, E.; Landrum, G.; Gaulton, A.; Atkinson, F.; Bellis, L. J.; Veij, M. D.; Leach, A. R. An open source chemical structure curation pipeline using RDKit. *Journal of Cheminformatics* **2020**, *12*, 51.
- (46) Kudo, T. Subword Regularization: Improving Neural Network Translation Models with Multiple Subword Candidates. *ACL 2018 - 56th Annual Meeting of the Association for Computational Linguistics, Proceedings of the Conference (Long Papers)* **2018**, *1*, 66–75.
- (47) Schwaller, P.; Laino, T.; Gaudin, T.; Bolgar, P.; Hunter, C. A.; Bekas, C.; Lee, A. A. Molecular Transformer: A Model for Uncertainty-Calibrated Chemical Reaction Prediction. *ACS Central Science* **2019**, *5*, 1572–1583.
- (48) Leon, M.; Perezhohin, Y.; Peres, F.; Popovič, A.; Castelli, M. Comparing SMILES and SELFIES tokenization for enhanced chemical language modeling. *Scientific Reports* **2024**, *14*, 25016.
- (49) Liu, Y.; Ott, M.; Goyal, N.; Du, J.; Joshi, M.; Chen, D.; Levy, O.; Lewis, M.; Zettlemoyer, L.; Stoyanov, V.; Allen, P. G. RoBERTa: A Robustly Optimized BERT Pre-training Approach. **2019**, Preprint at <https://arxiv.org/abs/1907.11692v1>.
- (50) Yang, Z.; Dai, Z.; Yang, Y.; Carbonell, J.; Salakhutdinov, R.; Le, Q. V. XLNet: Generalized Autoregressive Pretraining for Language Understanding. *Advances in Neural Information Processing Systems* **2019**, *32*, Preprint at <https://arxiv.org/abs/1906.08237v2>.

Extended Data:

BERTology of Molecular Property Prediction

Mohammad Mostafanejad,^{*,†,‡} Paul Saxe,^{*,†,‡} and T. Daniel Crawford^{*,†,‡}

[†]*Department of Chemistry, Virginia Tech, Blacksburg, Virginia 24061, USA*

[‡]*Molecular Sciences Software Institute, Blacksburg, Virginia 24060, USA*

E-mail: smostafanejad@vt.edu; psaxe@vt.edu; crawdad@vt.edu

Table 1: Variations of the masked language modeling performance metrics with using different model weight initialization and data sampling random seeds^a

BERT Variant	(Model,Data) Seed	T-Loss ↓ ^c	V-Loss ↓ ^c	V-Acc ↑ ^c	V-wF1 ↑ ^c	V-PPPL ↓ ^c
Tiny	(1234,1234)	0.6483	0.4664	0.8793	0.8637	1.5943
Tiny	(1234,2345)	0.6560	0.4727	0.8783	0.8658	1.6042
Tiny	(1234,3456)	0.6449	0.4663	0.8930	0.8799	1.5941
Tiny	(2345,1234)	0.6449	0.4669	0.8823	0.8703	1.5950
Tiny	(3456,1234)	0.6613	0.4755	0.8786	0.8634	1.6088
$\bar{x} \pm s_N$		0.6511 ± 0.0073	0.4696 ± 0.0043	0.8823 ± 0.0062	0.8686 ± 0.0069	1.5993 ± 0.0068
Small	(1234,1234)	0.2352	0.1835	0.9461	0.9417	1.2014
Small	(1234,2345)	0.2359	0.1844	0.9338	0.9281	1.2025
Small	(1234,3456)	0.2353	0.1836	0.9502	0.9454	1.2015
Small	(2345,1234)	0.2359	0.1841	0.9402	0.9375	1.2021
Small	(3456,1234)	0.2342	0.1826	0.9565	0.9532	1.2004
$\bar{x} \pm s_N$		0.2353 ± 0.0007	0.1836 ± 0.0007	0.9453 ± 0.0088	0.9412 ± 0.0093	1.2016 ± 0.0008
Base^b	(1234,1234)	1.3880	4.7239	0.1301	0.0299	112.61
Base	(1234,2345)	0.1775	0.1357	0.9557	0.9528	1.1454
Base	(1234,3456)	0.1777	0.1359	0.9617	0.9575	1.1456
Base	(2345,1234)	0.1782	0.1350	0.9619	0.9587	1.1446
Base	(3456,1234)	0.1781	0.1368	0.9588	0.9567	1.1465
$\bar{x} \pm s_N$		0.1779 ± 0.0003	0.1359 ± 0.0007	0.9595 ± 0.0029	0.9564 ± 0.0026	1.1455 ± 0.0008

^a The entire PubChem (ver. 04/18/2025) dataset (119,184,806 entries) is randomly split into training (95,347,844 entries amounting to 80% of the data) and validation (23,836,962 data points which counts as 20% of the data) sets.

^b The model diverges during training and the behavior is persistent over several runs. As such, this experiment is excluded from calculating the mean (\bar{x}) and standard deviation (s_N).

^c ↑: higher is better; ↓: lower is better.

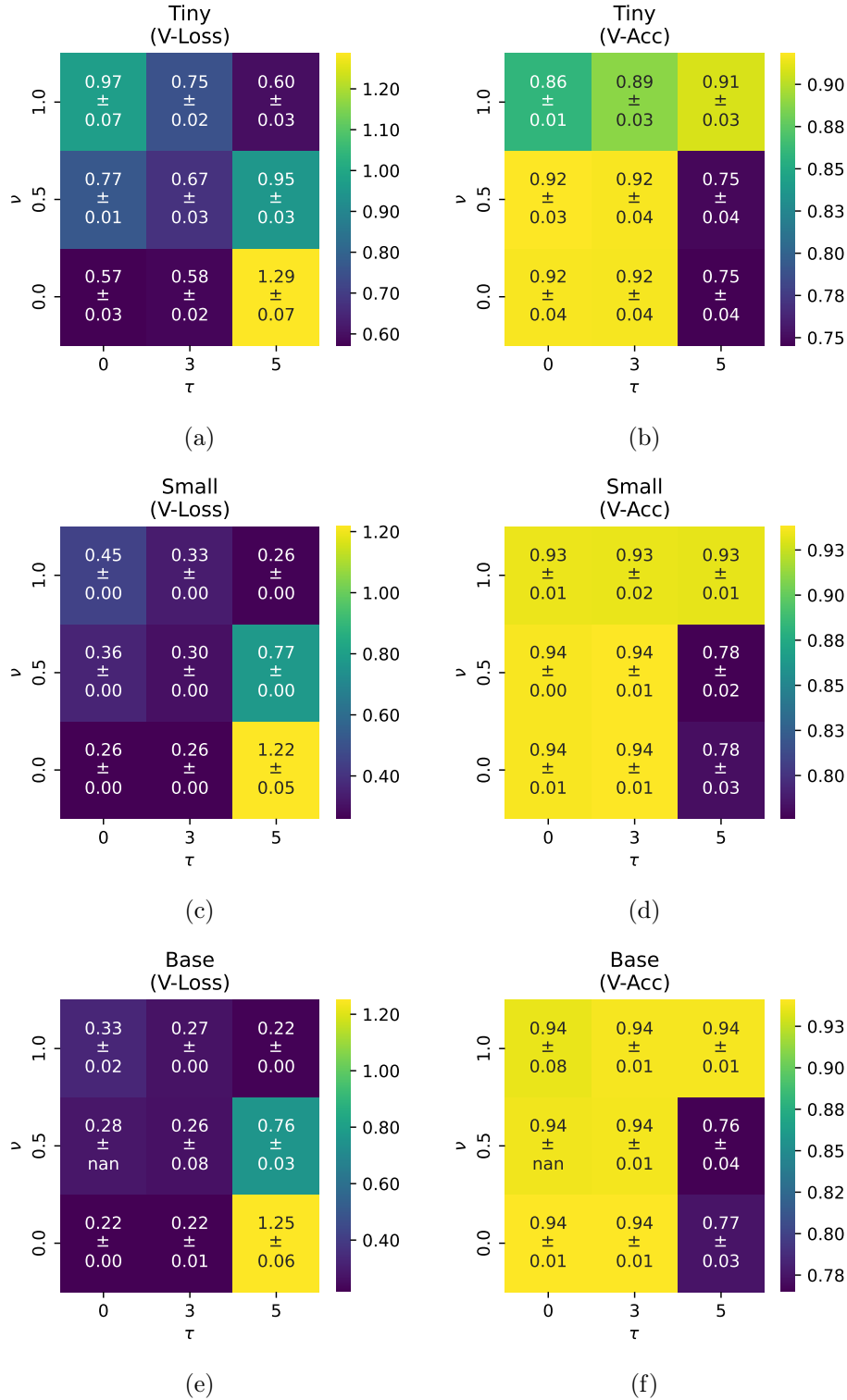


Figure 1: The effect of standardization noise on the pre-training validation loss (a,c,e) and accuracy (b,d,f) of BERT for masked language modeling. Both metrics are averaged over three independent runs with different data sampling and model initialization seeds. The error bars are based on 95% confidence interval which are not defined (NaN) for samples of $N = 1$ runs, if the other two have diverged and removed from the calculating the statistical summaries. See Supporting Information for more details.

Table 2: Variations of the masked language modeling performance metrics, for pre-training multiple variants of BERT on canonical isomeric SMILES from the PubChem (ver. 04/18/2025) dataset, tokenized with various tokenization algorithms^a

BERT Variant	(Model,Data) Seed	Tokenizer	T-Loss ↓ ^c	V-Loss ↓ ^c	V-Acc ↑ ^c	V-wF1 ↑ ^c	V-PPPL ↓ ^c
Tiny	(1234,1234)	WordPiece	0.6483	0.4664	0.8793	0.8637	1.5943
Tiny	(1234,2345)	WordPiece	0.6560	0.4727	0.8783	0.8658	1.6042
Tiny	(2345,1234)	WordPiece	0.6449	0.4669	0.8823	0.8703	1.5950
	$\bar{x} \pm s_N$		0.6497 ± 0.0057	0.4687 ± 0.0035	0.8800 ± 0.0021	0.8866 ± 0.0033	1.5978 ± 0.0056
Small	(1234,1234)	WordPiece	0.2352	0.1835	0.9461	0.9417	1.2014
Small	(1234,2345)	WordPiece	0.2359	0.1844	0.9338	0.9281	1.2025
Small	(2345,1234)	WordPiece	0.2359	0.1841	0.9402	0.9375	1.2021
	$\bar{x} \pm s_N$		0.2357 ± 0.0004	0.1840 ± 0.0005	0.9400 ± 0.0062	0.9358 ± 0.0070	1.2020 ± 0.0006
Base^b	(1234,1234)	WordPiece	1.388	4.724	0.1301	0.02994	112.61
Base	(1234,2345)	WordPiece	0.1357	0.1775	0.9557	0.9528	1.1454
Base	(2345,1234)	WordPiece	0.1782	0.1350	0.9619	0.9587	1.1446
	$\bar{x} \pm s_N$		0.1569 ± 0.0300	0.1562 ± 0.0300	0.9588 ± 0.0044	0.9557 ± 0.0042	1.1450 ± 0.0006
Tiny	(1234,1234)	BPE	0.5982	0.4430	0.8652	0.8520	1.5574
Tiny	(1234,2345)	BPE	0.5803	0.4258	0.8743	0.8611	1.5308
Tiny	(2345,1234)	BPE	0.5867	0.4333	0.8762	0.8664	1.5423
	$\bar{x} \pm s_N$		0.5884 ± 0.0090	0.4340 ± 0.0086	0.8719 ± 0.0058	0.8599 ± 0.0073	1.5435 ± 0.0133
Small	(1234,1234)	BPE	0.2031	0.1597	0.9410	0.9374	1.1731
Small	(1234,2345)	BPE	0.2075	0.1626	0.9452	0.9422	1.1766
Small	(2345,1234)	BPE	0.2067	0.1620	0.9467	0.9441	1.1759
	$\bar{x} \pm s_N$		0.2058 ± 0.0023	0.1614 ± 0.0015	0.9443 ± 0.0030	0.9412 ± 0.0034	1.1752 ± 0.0018
Base	(1234,1234)	BPE	0.1513	0.1171	0.9554	0.9537	1.1243
Base^b	(1234,2345)	BPE	1.457	4.130	0.1076	0.02092	62.180
Base	(2345,1234)	BPE	0.1499	0.1154	0.9573	0.9554	1.1223
	$\bar{x} \pm s_N$		0.1506 ± 0.0010	0.1163 ± 0.0012	0.9563 ± 0.0013	0.9546 ± 0.0012	1.1233 ± 0.0014

^a The entire PubChem (ver. 04/18/2025) dataset (119,184,806 entries) is randomly split into training (95,347,844 entries amounting to 80% of the data) and validation (23,836,962 data points which counts as 20% of the data) sets.

^b The model diverges during training and the behavior is persistent over several runs. As such, this experiment is excluded from calculating the mean (\bar{x}) and standard deviation (s_N).

^c ↑: higher is better; ↓: lower is better.

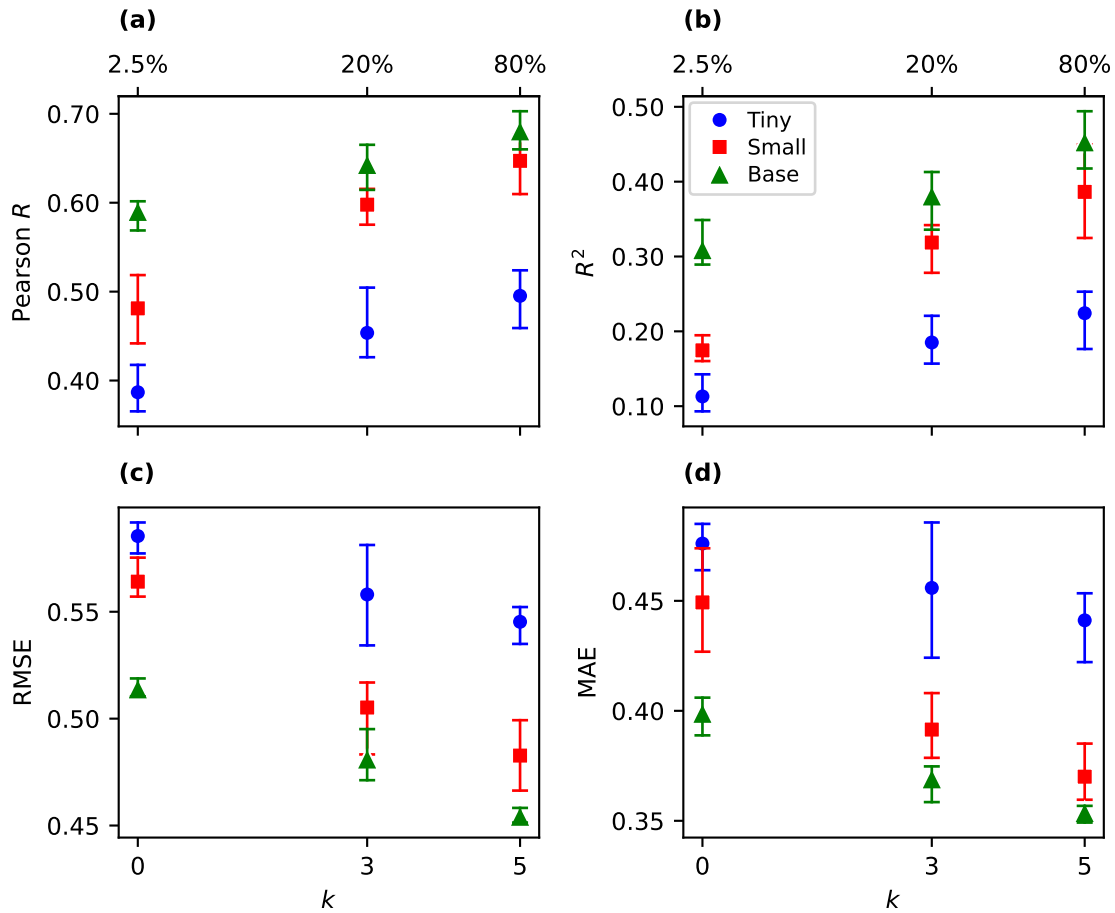


Figure 2: Variations of BERT’s 3-fold cross-validation fine-tuning metrics, (a) Pearson R , (b) R^2 , (c) RMSE, (d) MAE, versus the pre-training dataset size bin index, k , for the HLM endpoint (the corresponding data percentages are shown on the top axes). A hyperparameter search of 50 models is performed on each fold for each model variant and dataset size bin index and the best model is selected based on the validation R^2 , following Ref. 1

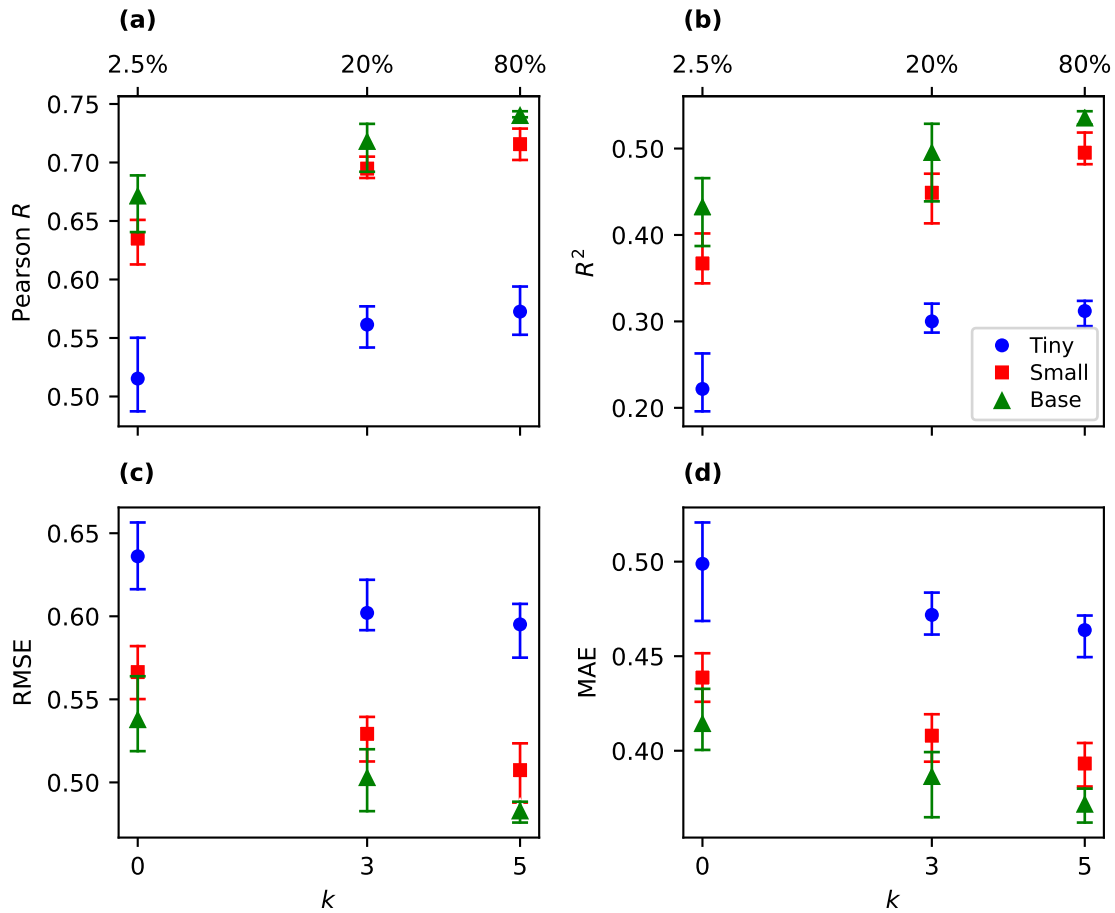


Figure 3: Variations of BERT’s 3-fold cross-validation fine-tuning metrics, (a) Pearson R , (b) R^2 , (c) RMSE, (d) MAE, versus the pre-training dataset size bin index, k , for the hPPB endpoint (the corresponding data percentages are shown on the top axes). A hyperparameter search of 50 models is performed on each fold for each model variant and dataset size bin index and the best model is selected based on the validation R^2 , following Ref. 1

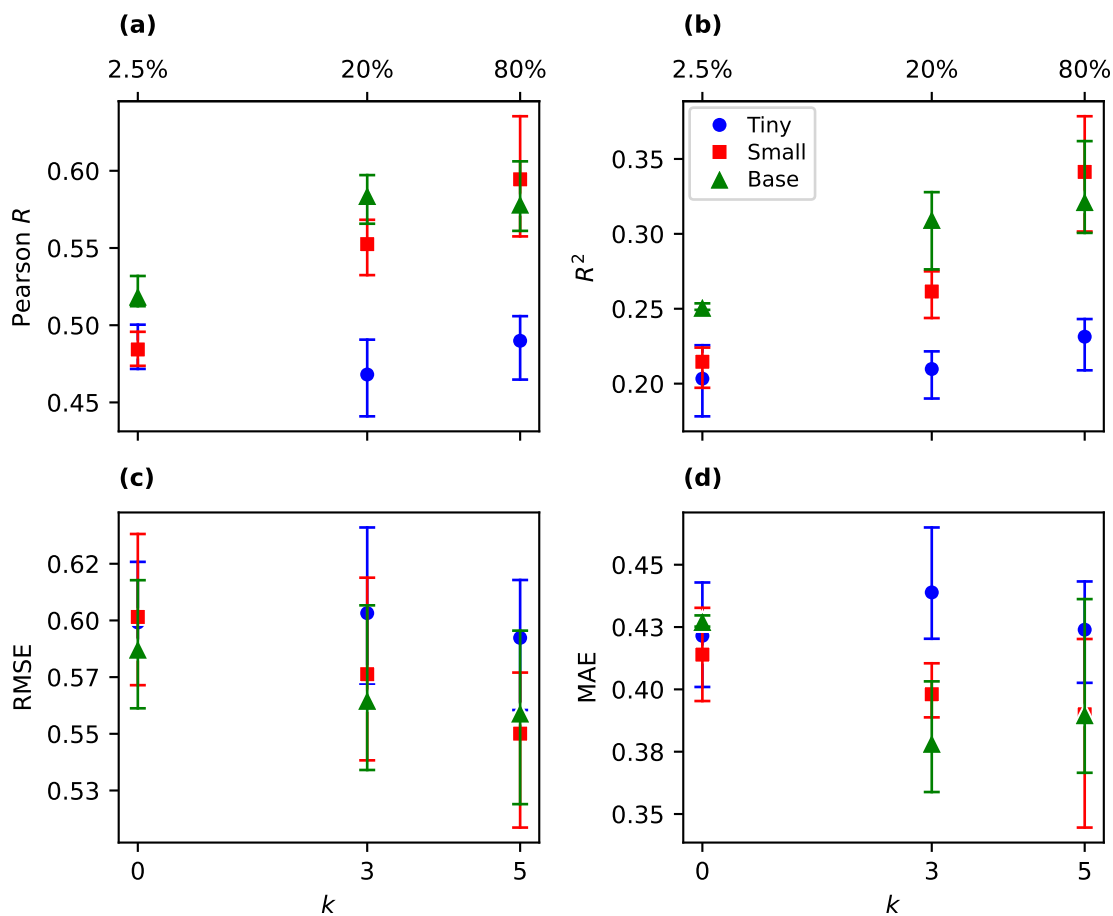


Figure 4: Variations of BERT’s 3-fold cross-validation fine-tuning metrics, (a) Pearson R , (b) R^2 , (c) RMSE, (d) MAE, versus the pre-training dataset size bin index, k , for the solubility endpoint (the corresponding data percentages are shown on the top axes). A hyperparameter search of 50 models is performed on each fold for each model variant and dataset size bin index and the best model is selected based on the validation R^2 , following Ref. 1

References

- (1) Fang, C.; Wang, Y.; Grater, R.; Kapadnis, S.; Black, C.; Trapa, P.; Sciabola, S. Prospective Validation of Machine Learning Algorithms for Absorption, Distribution, Metabolism, and Excretion Prediction: An Industrial Perspective. *Journal of Chemical Information and Modeling* **2023**, *63*, 3263–3274.

Supporting Information:

BERTology of Molecular Property Prediction

Mohammad Mostafanejad,^{*,†,‡} Paul Saxe,^{*,†,‡} and T. Daniel Crawford^{*,†,‡}

[†]*Department of Chemistry, Virginia Tech, Blacksburg, Virginia 24061, USA*

[‡]*Molecular Sciences Software Institute, Blacksburg, Virginia 24060, USA*

E-mail: smostafanejad@vt.edu; psaxe@vt.edu; crawdad@vt.edu

Contents

1	Computational Details	3
1.1	High-performance Compute Nodes and Accelerator Hardware	3
1.2	Global and Micro-Batch Sizes	3
2	The Effect of Standardization on Pre-training	4
2.1	Dataset Pre-processing	4
2.2	Molecular Sanitization in RDKit	4
2.3	A Primer on Standardization Protocols	6
2.4	Simulating the Standardization Noise in the PubChem Dataset	12
3	The Effect of Dataset and Model Sizes on Pre-training	17
4	Ablation Studies and Hyperparameter Tuning	20
4.1	Supervised fine-tuning on the Biogen ADME Dataset	20
4.2	Hyperparameter Search Spaces for Classical ML Models	24
4.3	Optimized Hyperparameters of the Fine-tuned Models	25
5	Budget and Cost Estimations	28
6	BERT Architectural Details	29
	References	30

1 Computational Details

1.1 High-performance Compute Nodes and Accelerator Hardware

All prototyping and initial testings are performed on an on-premise high-performance desktop machine with $2 \times$ NVIDIA A100 80GB PCIe4 graphics processing units (GPUs), awarded by NVIDIA Academic Hardware Grant Program. The production-ready scripts, pre-processed standardized data and all model artifacts are transferred to one of Virginia Tech’s Advanced Research Computing (ARC) flagship TinkerCliffs or Falcon compute cluster nodes for pre-training and fine-tuning. We pre-train the Tiny-Bidirectional Encoder Representations from Transformers (BERT) models using $16 \times$ NVIDIA A30 24GB GPUs on 4 Falcon nodes (each with 4 GPUs), the Small-BERT on $8 \times$ NVIDIA L40S 48GB GPUs on 2 Falcon nodes (each with 4 GPUs), and the Base-BERT models on $8 \times$ NVIDIA H200 141GB or NVIDIA A100 SMX4 80GB PCIe4 GPUs on 1 TinkerCliffs node (each with 8 GPUs) in distributed data parallel (DDP) mode. The effective global batch sizes of 1024 and 512 are adopted for pre-training and evaluation of all models, respectively (see Sec. 1.2 for more details). Subsequent fine-tunings and hyperparameter searches are performed on the same nodes but using a single GPU for each experiment.

1.2 Global and Micro-Batch Sizes

Since we use DDP alongside a wide range of nodes with different number of GPUs and GPU memory capacities in our experiments, we ensured that the effective global batch size (B_{eff}) remains the same across all experiments as it will be different from the adopted micro-batch size on each GPU, (B_{GPU}), through the following expression

$$B_{\text{eff}} = N_{\text{nodes}} \times N_{\text{GPU}} \times B_{\text{GPU}} \times N_{\text{GA}}. \quad (1)$$

Here, N_{nodes} is the number of nodes, N_{GPU} is the number of GPUs per node and N_{GA} is the number of gradient accumulation steps. For all our calculations, N_{GA} is set to 1.

2 The Effect of Standardization on Pre-training

2.1 Dataset Pre-processing

The Simplified Molecular Input Line Entry System (SMILES) string,

```
COC1=CC=C(C=C1)C2C3=C(C=CC4=CC=CC=C43)OC5=CC6=C(C=C5)C7
=NC8=C9C=CC1=CC9=C(N8)N=C3C4=C5C=CC(=C4)OC4=C(C(C8=C(C=CC9=CC=CC=C98)OC8
=CC9=C(C=C8)C8=NC9=NC9=C%10C=C(C=CC%10=C(N9)N=C9C%10=C(C=C(C=C%10)OC%10
=C2C2=CC=CC=C2C=C%10)C(=N9)NC2=NC(=N8)C8=C2C=C(C=C8)OC2=C(C(C8=C(C=CC9=CC
=CC=C98)OC8=CC9=C(C=C8)C(=NC5=N3)N=C9NC6=N7)C3=CC=C(C=C3)OC)C3=CC=CC=C3C
=C2)OC2=C(C(C3=C(O1)C=CC1=CC=CC=C13)C1=CC=C(C=C1)OC)C1=CC=CC=C1C=C2)C1=CC
=C(C=C1)OC)C1=CC=CC=C1C=C4
```

from the PubChem dataset (ver. 04/18/2025) cannot be processed by RDKit's `MolFromSmiles()` function raising the error:

Maximum BFS search size exceeded. This is likely due to a highly symmetric fused ring system.

As such, this SMILES is excluded from the dataset before proceeding to the standardization and tokenization steps.

2.2 Molecular Sanitization in RDKit

Since the ChEMBL standardization pipeline is based on RDKit, it is imperative to understand the concept of molecular sanitization. The content of this section closely follows the RDKit documentation on this topic.¹

All molecule parsing functions in RDKit perform a sanitization operation by default to

ensure that the generated molecules are accompanied by useful computed properties, such as hybridization, bond types *etc.* and can be represented by Lewis structures. The sanitization process in RDKit involves the following operations, performed in the order listed below:

- 1- `clearComputedProps`: Clears all existing computed properties on the molecule, its atoms and bonds. This operation is always performed in sanitization.
- 2- `cleanUp`: standardizes the valence states in the following substructures:
 - Neutral 5-valent nitrogen atoms connected to neighboring oxygens with double bonds or nitrogens with triple bonds are converted to their zwitterionic form. For example, $\text{N}(=\text{O})(=\text{O})$ and $\text{C}-\text{N}=\text{N}\#\text{N}$ are converted to $[\text{N}^+](=\text{O})[\text{O}^-]$ and $\text{C}-\text{N}=[\text{N}^+]=[\text{N}^-]$, respectively,
 - neutral 5-valent phosphorous atom connected to a neighboring oxygen with a double bond and another carbon or phosphorous atom is converted to its zwitterionic form. For example, $\text{C}=\text{P}(=\text{O})\text{O}$ is converted to $\text{C}=[\text{P}^+](\text{O}^-)\text{O}$,
 - neutral 3-, 5-, or 7-valent chlorine, bromine, or iodine atoms connected to neighboring oxygens are converted to their zwitterionic form. For example, $\text{O}=\text{Cl}(=\text{O})=\text{O}$ is converted to $[\text{O}^-][\text{Cl}^{+2}](\text{O}^-)\text{O}$.

The aforementioned operations will not raise any exceptions.

- 3- `cleanUpOrganometallics`: converts single bonds between a metal and hypervalent atom in organometallics to a dative bond,
- 4- `updatePropertyCache`: computes the explicit and implicit valencies on all atoms in the structure. This operation is always performed by default but if skipped, non-standard valencies will not be tested,
- 5- `symmetrizeSSSR`: performs the symmetrized smallest set of smallest rings (SSSR) algorithm,

- 6- `Kekulize`: converts aromatic rings to their Kekulé form. This operation will raise an exception if the algorithm fails to Kekulize a ring or if aromatic bonds are found outside of rings.
- 7- `assignRadicals`: determines the number of radical electrons, if any, on each atom,
- 8- `setAromaticity`: identifies the aromatic rings and ring systems, sets the aromaticity flag on atoms and bonds, and converts the pertinent bond orders to aromatic,
- 9- `setConjugation`: identifies the conjugated bonds,
- 10- `setHybridization`: assigns the hybridization state to each atom,
- 11- `cleanupChirality`: removes the chirality flag from non-*sp*³ atoms,
- 12- `adjustHs`: adds explicit hydrogens to preserve the chemistry, typically for heteroatoms in aromatic rings. The nitrogen atom in pyrrole offers an example for this operation.
- 13- `updatePropertyCache`: is used to recompute the explicit and implicit valencies on all atoms to capture non-physical valencies on atoms with aromatic flags that are accepted in the previous steps.

Finer control over the individual steps is offered by `rdkit.Chem.rdmolops.SanitizeMol()` and `rdkit.Chem.SanitizeFlags`.

2.3 A Primer on Standardization Protocols

Standardization protocols are workflows that process the chemical representation of compounds, such as SMILES, for an intended use. PubChem and ChEMBL databases have their own standardization and curation pipelines which ensure the uniqueness of the compounds and their usefulness for the potential downstream applications. Standardization protocols must clearly delineate their strategy about processing some of the key aspects of

the chemical representations, such as explicit or implicit specification of hydrogen atoms or handling of the stereo-centers.

Tautomerism, mesomerism and alternate ionization states can also contribute to the number of possible valid, non-identical representations of the same structure, which often exist in equilibrium. As such, tautomerism and the choice of the predominant variants of a structure can heavily impact the corresponding computed properties such as structural similarity, biological activity, as well as topological and physicochemical features.

Aromaticity is another aspect that can be defined in a multitude of ways, based on various criteria such as chemical behavior, energetic properties, magnetic effects, and structural traits. Different tools adopt different aromaticity models and in the absence of a standard definition of aromaticity, it is typically perceived from a Kekulé structure. However, the best standardization approach may need to handle aromaticity and tautomerism together, as the choice of a canonical tautomeric form may directly affect aromaticity, depending on the aromaticity model employed.

The ChEMBL curation and standardization pipeline² (Fig. 1) is based on `RDKit` and has three components: (i) `Checker` which tests the validity of the chemical structures and flags any serious errors, (ii) `Standardizer` which formats compounds according to a predefined set of rules and conventions, and (iii) `GetParent` which removes any salts and solvents from the compound to create its parent structure, with the exception of salts in organometallic compounds. The list of salts used in ChEMBL is an extension of USAN Council’s list of pharmacological salts. The `GetParent` module also removes all isotopic information from the representation.²

ChEMBL standardization pipeline uses International Chemical Identifiers (InChIs) and the corresponding hashed InChI keys as a measure of uniqueness for the chemical structures calculated from the `molfiles` using the `InChI Trust 1.05` software. Canonical SMILES are used as a secondary representation of the chemical structures. Note that V2000 `molfiles` cannot distinguish between relative and absolute stereochemistry but V3000 `molfiles` can.

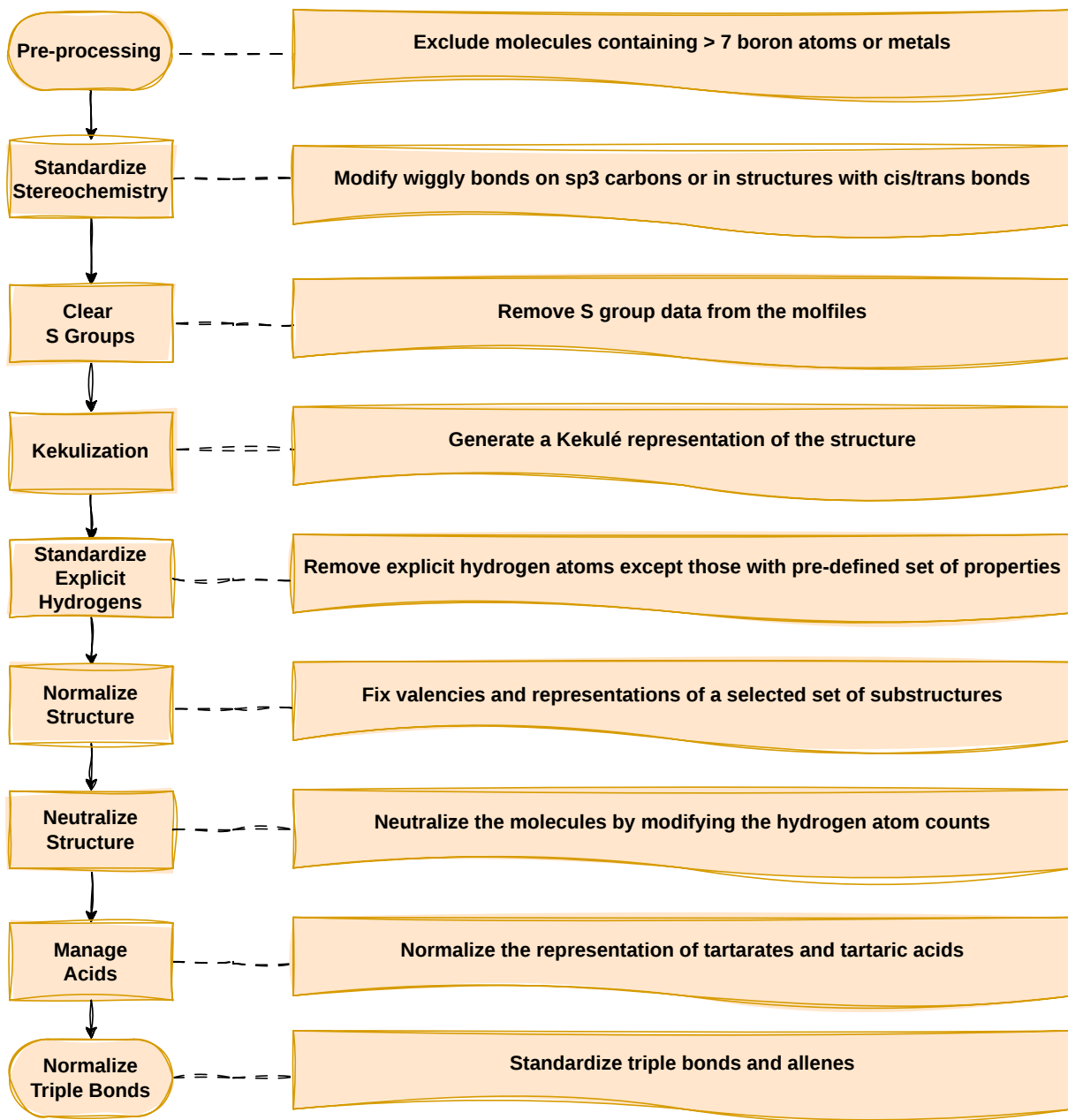


Figure 1: ChEMBL standardization protocol

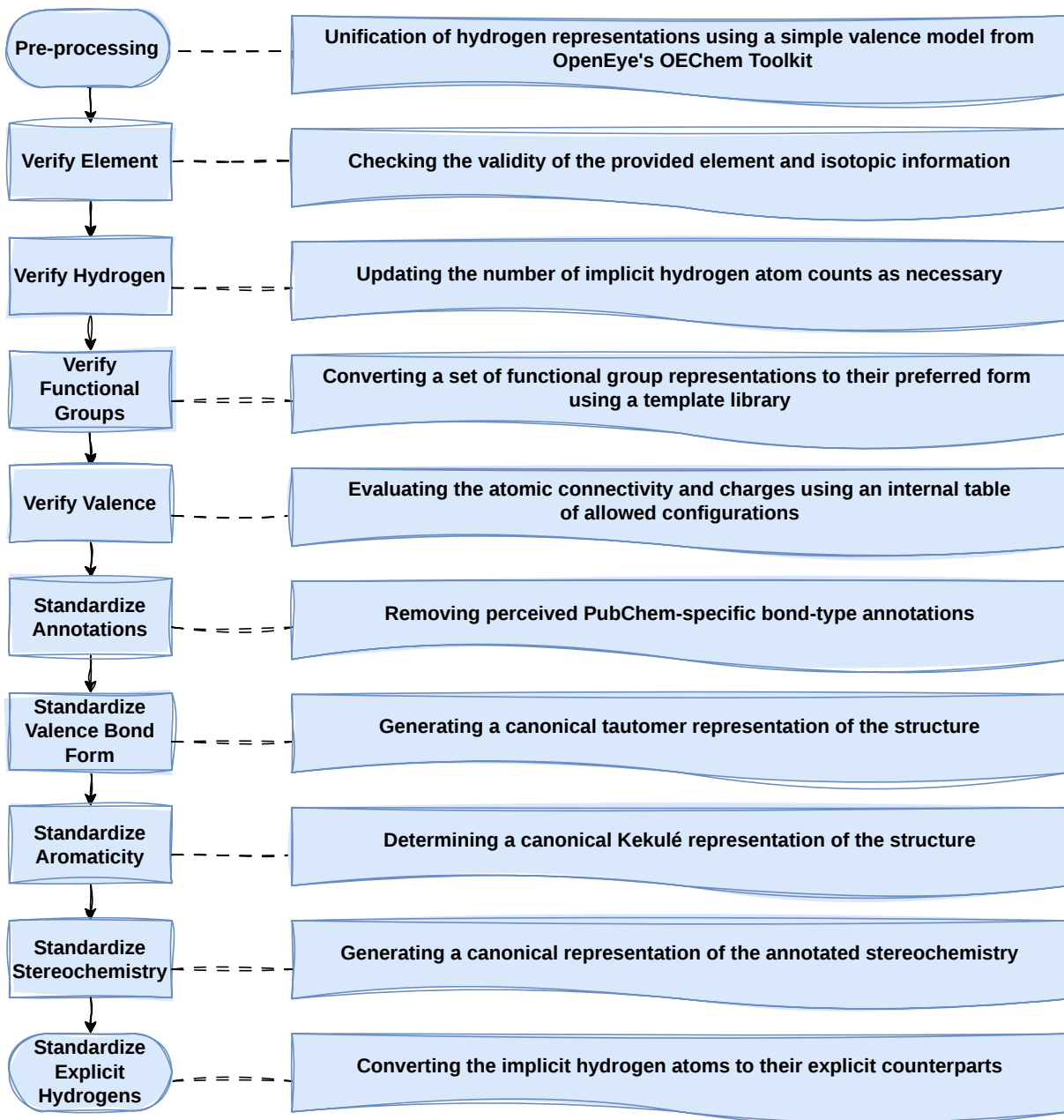


Figure 2: PubChem standardization protocol

Also, unlike `molfiles` and SMILES, InChIs are designed as an identifier not a structural format, suitable for cheminformatics applications. For example, the standard InChI representation is independent of the tautomeric form. Thus, different tautomers of a compound will have identical standard InChIs. Also, InChIs do not distinguish between *cis*/*trans* form of organometallic compounds such as *cis*-/*trans*-platinum.

PubChem standardization protocol (Fig. 2), on the other hand, uses canonical isomeric SMILES to identify the unique structures as this method is proven to generate more unique structures than just using standard InChIs.³ While the PubChem protocol provides canonical tautomeric forms for their compounds, the ChEMBL protocol cites three reasons not to. The developers of ChEMBL protocol rely on medicinal chemists to assign the most appropriate tautomeric form to their compounds which is consistent with the target application. Furthermore, tautomers can inter-convert under experimental conditions. Moreover, changing the tautomeric form can change the stereochemistry by modifying the chiral centers. For example, thalidomide can inter-convert between the therapeutic *R*-enantiomer and teratogenic *S*-enantiomer through enol tautomerism.

Regardless of the aforementioned technicalities, the standardization protocols can have important practical implications for the performance downstream models for molecular property prediction (MPP) tasks. For example, the ChEMBL standardization pipeline involves the removal of a pre-defined set of salts and solvents. This means that a model trained on ChEMBL-standardized data may not perform well for property prediction tasks such as predicting toxicity values if the non-standardized SMILES forms are not available in the training data. For example, 2,4,5-trimethylaniline and its hydrochloride form, which are not differentiated after ChEMBL standardization, have carcinogenic potency tumor dose (TD_{50}) values of 33.6 and 98.5 mg per kg body weight per day in rats, respectively.⁴ The TD_{50} value is the chronic dose-rate that would induce tumors in half of the test population at the end of their standard lifespan.

In order to further illustrate the importance of standardization in the context of training

large language models (LLMs) for MPP tasks, we provide a brief example to demonstrate its potential impact on various steps of the natural language processing (NLP) workflows. Let us consider five chemical compounds with their corresponding standardized SMILES representations, shown in Table 1.

Table 1: The SMILES representation of five different compounds standardized by PubChem and ChEMBL protocols

PubChem	ChEMBL
<chem>CC(=O)[O-]</chem>	<chem>CC(=O)O</chem>
<chem>O=[As]([O-])([O-])O</chem>	<chem>O=[As](O)(O)O</chem>
<chem>[NH4+]</chem>	<chem>N</chem>
<chem>[CH3-]</chem>	<chem>C</chem>
<chem>CS(C)=O</chem>	<chem>C[S+](C)[O-]</chem>

Looking at the first pair of rows in Table 1 and considering the standardization workflows in Figs. 1 and 2, one can show that the PubChem pipeline preserves the anionic forms of the functional groups while the ChEMBL pipeline neutralizes them. In the fifth row, PubChem standardization preserves the neutral form of S=O with a double-bond while ChEMBL standardization generates a charge-separated zwitterionic form with S⁺ and O⁻. The decision making behind the design of both PubChem and ChEMBL standardization pipelines can become more clear if one considers the fact that the former uses OpenEye’s `OEChem` toolkit (commercial and closed-source) for processing the SMILES while the latter employs `RDKit` (free and open-source). Both software packages have their own unique features and capabilities for handling the SMILES representation of chemical structures.

From the aforementioned examples, it becomes evident that the choice of standardization pipeline can yield different vocabularies with unique token frequencies and distributions which can potentially lead to distinct tokenization, embedding and ultimately pre-training and fine-tuning outcomes.

2.4 Simulating the Standardization Noise in the PubChem

Dataset

In order to study the impact of standardization noise on the pre-training performance of BERT, we create six data bins within the PubChem dataset, each with different sizes (Fig. 3), and gradually replace the PubChem canonical isomeric SMILES with their ChEMBL standardized counterparts.

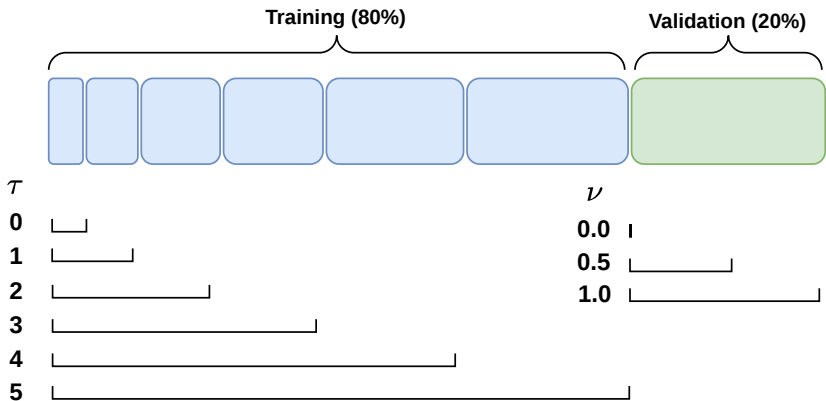


Figure 3: Corrupting the PubChem dataset with ChEMBL standardized SMILES

First, the PubChem dataset is shuffled and randomly split into training and validation splits with sizes $N_{\text{train}} = 95,347,844$ and $N_{\text{valid}} = 23,836,962$, respectively. The data corruption within each split is subsequently controlled by two parameters, τ and ν , according to the following expressions

$$N_{\text{train}}^{\text{C}} = a \times 2^{\tau} + b, \quad (2a)$$

$$N_{\text{train}}^{\text{P}} = N_{\text{train}} - N_{\text{train}}^{\text{C}}, \quad (2b)$$

$$N_{\text{valid}}^{\text{C}} = \nu \times N_{\text{valid}}, \quad (2c)$$

$$N_{\text{valid}}^{\text{P}} = N_{\text{valid}} - N_{\text{valid}}^{\text{C}}. \quad (2d)$$

Here, $\tau = 0, 1, 2, \dots, 5$ and $\nu = 0.0, 0.5$ and 1.0 correspond the portions of the training

and validation data splits, in which the PubChem standardized canonical isomeric SMILES are replaced with those standardized by the ChEMBL standardization pipeline. Also, $a = 2,979,620$ is the size of the first bin and b is the correction factor which ensures that the addition of the sixth bin ($\tau = 5$) will cover 80% of the PubChem dataset. As such, $b = 4$ when $\tau = 5$ and zero otherwise. The superscripts C and P in N^C and N^P correspond to the ChEMBL and PubChem standardized data, respectively. We run each pre-training experiment three times with different model initialization and data sampling seeds and present the results in Table 2.4.

Some of the entries in Table 2.4 are shown in red to denote runs which resulted in model divergences or stopped by the early-stopping conditions. For a convenient interpretation of the data, we illustrate the statistical summaries in Table 2.4 as heatmaps and present them in the main text and the Extended Data section.

Table 2: Variations of the pre-training performance of BERT versus the SMILES standardization noise

BERT (Model,Data)		Epochs	τ^a	ν^a	T-Loss	\downarrow^d V-Loss	\downarrow^d V-Acc	\uparrow^d V-wF1	\uparrow^d V-PPPL	\downarrow^d
Variant	Seeds									
Tiny	(1234,1234)	10	0	0.0	0.5721	0.5851	0.9090	0.9027	1.7952	
Tiny	(1234,2345)	10	0	0.0	0.5644	0.5718	0.9065	0.9023	1.7714	
Tiny	(2345,1234)	10	0	0.0	0.5527	0.5585	0.9337	0.9329	1.7480	
	\bar{x}				0.5631	0.5718	0.9164	0.9126	1.7715	
	s_N				0.0098	0.0133	0.0150	0.0175	0.0236	
Tiny	(1234,1234)	10	0	0.5	0.5628	0.7640	0.9142	0.9091	2.1468	
Tiny	(1234,2345)	10	0	0.5	0.5673	0.7647	0.9071	0.9025	2.1483	
Tiny	(2345,1234)	10	0	0.5	0.5690	0.7698	0.9337	0.9324	2.1593	
	\bar{x}				0.5664	0.7662	0.9183	0.9147	2.1515	
	s_N				0.0032	0.0032	0.0138	0.0157	0.0068	
Tiny	(1234,1234)	10	0	1.0	0.5481	0.9467	0.8549	0.8419	2.5772	
Tiny	(1234,2345)	10	0	1.0	0.5587	0.9651	0.8555	0.8415	2.6251	
Tiny	(2345,1234)	10	0	1.0	0.5583	1.002	0.8644	0.8517	2.7224	
	\bar{x}				0.5550	0.9711	0.8582	0.8450	2.6416	
	s_N				0.0060	0.0279	0.0053	0.0058	0.0740	
Tiny	(1234,1234)	10	3	0.0	0.6109	0.5901	0.9097	0.9024	1.8041	
Tiny	(1234,2345)	10	3	0.0	0.6038	0.5839	0.9052	0.8990	1.7930	
Tiny	(2345,1234)	10	3	0.0	0.5934	0.5736	0.9337	0.9301	1.7747	

Table 1: Variations of the pre-training performance of BERT versus the SMILES standardization noise (continued)

BERT (Model,Data)		Epochs	τ^a	ν^a	T-Loss \downarrow^d	V-Loss \downarrow^d	V-Acc \uparrow^d	V-wF1 \uparrow^d	V-PPPL \downarrow^d
Variant	Seeds								
	\bar{x}				0.6027	0.5825	0.9162	0.9105	1.7906
	s_N				0.0088	0.0083	0.0153	0.0170	0.0149
Tiny	(1234,1234)	10	3	0.5	0.5974	0.6621	0.9071	0.9016	1.9388
Tiny	(1234,2345)	10	3	0.5	0.6180	0.6796	0.9071	0.8977	1.9731
Tiny	(2345,1234)	10	3	0.5	0.6186	0.6830	0.9362	0.9321	1.9799
	\bar{x}				0.6114	0.6749	0.9168	0.9105	1.9639
	s_N				0.0121	0.0112	0.0168	0.0188	0.0220
Tiny	(1234,1234)	10	3	1.0	0.6007	0.7424	0.8908	0.8803	2.1009
Tiny	(1234,2345)	10	3	1.0	0.6072	0.7566	0.8735	0.8637	2.1310
Tiny	(2345,1234)	10	3	1.0	0.5908	0.7547	0.9004	0.8903	2.1270
	\bar{x}				0.5996	0.7512	0.8882	0.8781	2.1196
	s_N				0.0083	0.0077	0.0136	0.0134	0.0163
Tiny^b	(1234,1234)	6	5	0.0	0.6166	1.256	0.7537	0.7588	3.5113
Tiny^b	(1234,2345)	4	5	0.0	0.6773	1.310	0.7267	0.7239	3.7063
Tiny^b	(2345,1234)	5	5	0.0	0.6450	1.294	0.7558	0.7562	3.6480
	\bar{x}				0.6463	1.2867	0.7454	0.7463	3.6218
	s_N				0.0304	0.0278	0.0163	0.0195	0.1001
Tiny	(1234,1234)	10	5	0.5	0.6080	0.9488	0.7290	0.7335	2.5826
Tiny	(1234,2345)	10	5	0.5	0.6004	0.9394	0.7572	0.7585	2.5584
Tiny	(2345,1234)	10	5	0.5	0.6101	0.9657	0.7599	0.7678	2.6267
	\bar{x}				0.6062	0.9513	0.7487	0.7533	2.5892
	s_N				0.0051	0.0133	0.0171	0.0177	0.0346
Tiny	(1234,1234)	10	5	1.0	0.5793	0.5853	0.9055	0.8996	1.7956
Tiny	(1234,2345)	10	5	1.0	0.6076	0.6113	0.8981	0.8893	1.8427
Tiny	(2345,1234)	10	5	1.0	0.5974	0.5985	0.9194	0.9114	1.8193
	\bar{x}				0.5948	0.5983	0.9077	0.9001	1.8192
	s_N				0.0143	0.0130	0.0108	0.0111	0.0236
Small	(1234,1234)	10	0	0.0	0.2192	0.2596	0.9386	0.9384	1.2964
Small	(1234,2345)	10	0	0.0	0.2198	0.2601	0.9399	0.9410	1.2971
Small	(2345,1234)	10	0	0.0	0.2201	0.2607	0.9301	0.9276	1.2978
	\bar{x}				0.2197	0.2601	0.9362	0.9357	1.2971
	s_N				0.0004	0.0005	0.0054	0.0071	0.0007
Small	(1234,1234)	10	0	0.5	0.2207	0.3573	0.9361	0.9373	1.4295
Small	(1234,2345)	10	0	0.5	0.2196	0.3560	0.9361	0.9361	1.4277
Small	(2345,1234)	10	0	0.5	0.2189	0.3544	0.9373	0.9354	1.4253
	\bar{x}				0.2197	0.3559	0.9365	0.9363	1.4275
	s_N				0.0009	0.0015	0.0007	0.0009	0.0021

Table 1: Variations of the pre-training performance of BERT versus the SMILES standardization noise (continued)

BERT (Model,Data)		Epochs	τ^a	ν^a	T-Loss \downarrow^d	V-Loss \downarrow^d	V-Acc \uparrow^d	V-wF1 \uparrow^d	V-PPPL \downarrow^d
Variant	Seeds								
Small	(1234,1234)	10	0	1.0	0.2188	0.4468	0.9302	0.9347	1.5633
Small	(1234,2345)	10	0	1.0	0.2206	0.4476	0.9315	0.9361	1.5646
Small	(2345,1234)	10	0	1.0	0.2200	0.4468	0.9376	0.9406	1.5633
	\bar{x}				0.2198	0.4471	0.9331	0.9371	1.5638
	s_N				0.0009	0.0005	0.0039	0.0031	0.0008
Small	(1234,1234)	10	3	0.0	0.2272	0.2623	0.9418	0.9416	1.2999
Small	(1234,2345)	10	3	0.0	0.2268	0.2620	0.9374	0.9360	1.2996
Small	(2345,1234)	10	3	0.0	0.2268	0.2626	0.9346	0.9329	1.3003
	\bar{x}				0.2269	0.2623	0.9379	0.9368	1.2999
	s_N				0.0002	0.0003	0.0036	0.0044	0.0003
Small	(1234,1234)	10	3	0.5	0.2270	0.3004	0.9399	0.9409	1.3503
Small	(1234,2345)	10	3	0.5	0.2256	0.2990	0.9393	0.9399	1.3485
Small	(2345,1234)	10	3	0.5	0.2265	0.2988	0.9340	0.9315	1.3482
	\bar{x}				0.2264	0.2994	0.9377	0.9374	1.3490
	s_N				0.0007	0.0008	0.0033	0.0052	0.0011
Small	(1234,1234)	10	3	1.0	0.2263	0.3311	0.9335	0.9332	1.3925
Small	(1234,2345)	10	3	1.0	0.2277	0.3335	0.9256	0.9276	1.3958
Small	(2345,1234)	10	3	1.0	0.2269	0.3336	0.9383	0.9392	1.3960
	\bar{x}				0.2269	0.3327	0.9325	0.9333	1.3948
	s_N				0.0007	0.0014	0.0064	0.0058	0.0020
Small ^b	(1234,1234)	4	5	0.0	0.2540	1.209	0.7893	0.8040	3.3516
Small ^b	(1234,2345)	4	5	0.0	0.2533	1.199	0.7900	0.7924	3.3178
Small ^b	(2345,1234)	5	5	0.0	0.2456	1.240	0.7667	0.7849	3.4556
	\bar{x}				0.2510	1.2163	0.7820	0.7937	3.3750
	s_N				0.0047	0.0212	0.0132	0.0097	0.0718
Small ^b	(1234,1234)	6	5	0.5	0.2380	0.7735	0.7825	0.7974	2.1674
Small ^b	(1234,2345)	7	5	0.5	0.2334	0.7742	0.7647	0.7829	2.1689
Small ^b	(2345,1234)	7	5	0.5	0.2339	0.7710	0.7811	0.7945	2.1620
	\bar{x}				0.2351	0.7729	0.7761	0.7916	2.1661
	s_N				0.0026	0.0017	0.0099	0.0077	0.0036
Small	(1234,1234)	10	5	1.0	0.2229	0.2650	0.9302	0.9314	1.3034
Small	(1234,2345)	10	5	1.0	0.2217	0.2645	0.9289	0.9301	1.3027
Small	(2345,1234)	10	5	1.0	0.2230	0.2654	0.9369	0.9369	1.3040
	\bar{x}				0.2225	0.2650	0.9320	0.9328	1.3034
	s_N				0.0007	0.0005	0.0043	0.0036	0.0006
Base	(1234,1234)	10	0	0.0	0.0139	0.2167	0.9437	0.9447	1.2420
Base	(1234,2345)	10	0	0.0	0.1676	0.2160	0.9405	0.9406	1.2411

Table 1: Variations of the pre-training performance of BERT versus the SMILES standardization noise (continued)

BERT (Model,Data)		Epochs	τ^a	ν^a	T-Loss \downarrow^d	V-Loss \downarrow^d	V-Acc \uparrow^d	V-wF1 \uparrow^d	V-PPPL \downarrow^d
Variant	Seeds								
Base	(2345,1234)	10	0	0.0	0.0138	0.2169	0.9386	0.9365	1.2422
	\bar{x}				0.0651	0.2165	0.9409	0.9406	1.2417
	s_N				0.0888	0.0005	0.0026	0.0041	0.0006
Base ^b	(1234,1234)	4	0	0.5	10.95	5.335	0.1466	0.03750	207.38
Base	(1234,2345)	10	0	0.5	0.0275	0.2774	0.9374	0.9380	1.3197
Base ^b	(2345,1234)	9	0	0.5	4.814	4.088	0.1327	0.03109	59.598
	\bar{x}				5.2651	3.2332	0.4056	0.3355	89.4321
	s_N				5.4772	2.6346	0.4606	0.5218	106.2198
Base ^{b,c}	(1234,1234)	4	0	1.0	23.94	4.158	0.1439	0.03622	63.969
Base	(1234,2345)	10	0	1.0	0.02779	0.3313	0.9289	0.9297	1.3928
Base	(2345,1234)	10	0	1.0	0.04259	0.3276	0.9417	0.9409	1.3876
	\bar{x}				0.0352	0.3294	0.9353	0.9353	1.3902
	s_N				0.0105	0.0027	0.0090	0.0079	0.0037
Base	(1234,1234)	10	3	0.0	0.1720	0.2168	0.9418	0.9433	1.2420
Base	(1234,2345)	10	3	0.0	0.02822	0.2177	0.9399	0.9407	1.2432
Base ^{b,c}	(2345,1234)	7	3	0.0	4.168	4.125	0.1434	0.03597	61.88
	\bar{x}				0.1001	0.2172	0.9409	0.9420	1.2426
	s_N				0.1017	0.0006	0.0013	0.0018	0.0008
Base	(1234,1234)	10	3	0.5	0.0140	0.2460	0.9399	0.9410	1.2789
Base	(1234,2345)	10	3	0.5	0.2256	0.2990	0.9393	0.9399	1.3485
Base	(2345,1234)	10	3	0.5	0.02847	0.2457	0.9353	0.9326	1.2785
	\bar{x}				0.0894	0.2636	0.9382	0.9379	1.3020
	s_N				0.1182	0.0307	0.0025	0.0046	0.0403
Base	(1234,1234)	10	3	1.0	0.1714	0.2675	0.9413	0.9411	1.3068
Base	(1234,2345)	10	3	1.0	0.01406	0.2688	0.9328	0.9340	1.3084
Base	(2345,1234)	10	3	1.0	0.1711	0.2682	0.9423	0.9432	1.3076
	\bar{x}				0.1188	0.2682	0.9388	0.9394	1.3076
	s_N				0.0907	0.0006	0.0052	0.0048	0.0008
Base ^b	(1234,1234)	4	5	0.0	0.2021	1.244	0.7853	0.7990	3.4711
Base ^b	(1234,2345)	4	5	0.0	0.1360	1.279	0.7629	0.7722	3.5929
Base ^b	(2345,1234)	4	5	0.0	0.2008	1.230	0.7741	0.7854	3.4200
	\bar{x}				0.1796	1.2510	0.7741	0.7855	3.4947
	s_N				0.0378	0.0253	0.0112	0.0134	0.0888
Base ^b	(1234,1234)	4	5	0.5	0.2020	0.7571	0.7820	0.7956	2.1321
Base ^b	(1234,2345)	5	5	0.5	0.1942	0.7442	0.7639	0.7817	2.1048
Base ^b	(2345,1234)	6	5	0.5	0.1892	0.7692	0.7487	0.7697	2.1581
	\bar{x}				0.1951	0.7569	0.7649	0.7823	2.1317

Table 1: Variations of the pre-training performance of BERT versus the SMILES standardization noise (continued)

BERT (Model,Data) Variant	Seeds	Epochs	τ^a	ν^a	T-Loss \downarrow^d	V-Loss \downarrow^d	V-Acc \uparrow^d	V-wF1 \uparrow^d	V-PPPL \downarrow^d
	s_N				0.0065	0.0125	0.0167	0.0130	0.0267
Base	(1234,1234)	10	5	1.0	0.1720	0.2234	0.9393	0.9391	1.2503
Base	(1234,2345)	10	5	1.0	0.0745	0.2229	0.9361	0.9376	1.2497
Base	(2345,1234)	10	5	1.0	0.0287	0.2234	0.9410	0.9404	1.2504
	\bar{x}				0.0917	0.2232	0.9388	0.9390	1.2501
	s_N				0.0732	0.0003	0.0025	0.0014	0.0004

^a τ and ν control the amount of standardization noise in the training and validation splits according to Eq. 2a-d.

^b The model diverges during training and/or stopped by the early stopping criterion.

^c The model is excluded from calculating the mean (\bar{x}) and standard deviation (s_N).

^d \uparrow : higher is better; \downarrow : lower is better.

3 The Effect of Dataset and Model Sizes on Pre-training

In order to study the dataset and model size effects on pre-training performance of BERT, we create six dataset bins with different sizes, where the number of training samples in each bin is defined as

$$N_{\text{train}} = a \times 2^k + b, \quad (3)$$

where $k = 0, 1, 2, 3, 4$ and 5 denotes the bin index, $a = 2,979,620$ is the size of the first bin and b is the correction factor which ensures that the addition of the sixth bin ($k = 5$) will cover 80% of the PubChem dataset. As such, $b = 4$ when $k = 5$ and zero otherwise.

Table 2: Variations of the pre-training performance of BERT versus dataset and model sizes

BERT (Model,Data) Variant	Seed	k^a	T-Loss \downarrow^d	V-Loss \downarrow^d	V-Acc \uparrow^d	V-wF1 \uparrow^d	V-PPPL \downarrow^d
Tiny	(1234,1234)	0	0.9602	1.3382	0.8618	0.8479	3.8123
Tiny	(1234,2345)	0	1.0184	1.3893	0.8606	0.8475	4.0122
Tiny	(2345,1234)	0	0.9708	1.3070	0.8650	0.8482	3.6950
	\bar{x}		0.9831	1.3449	0.8625	0.8479	3.8398
	s_N		0.0310	0.0416	0.0023	0.0004	0.1604
Tiny	(1234,1234)	1	0.7694	1.1407	0.8788	0.8681	3.1290

Table 1: Variations of the pre-training performance of BERT versus dataset and model sizes (continued)

BERT Variant	(Model,Data) Seed	k^a	T-Loss \downarrow^d	V-Loss \downarrow^d	V-Acc \uparrow^d	V-wF1 \uparrow^d	V-PPPL \downarrow^d
Tiny	(1234,2345)	1	0.7847	1.1735	0.8825	0.8694	3.2332
Tiny	(2345,1234)	1	0.7895	1.1738	0.8745	0.8607	3.2343
	\bar{x}		0.7812	1.1627	0.8786	0.8660	3.1988
	s_N		0.0105	0.0190	0.0040	0.0046	0.0605
Tiny	(1234,1234)	2	0.6798	0.8764	0.9026	0.8952	2.4023
Tiny	(1234,2345)	2	0.6691	0.8736	0.8926	0.8858	2.3956
Tiny	(2345,1234)	2	0.6715	0.8633	0.9037	0.8942	2.3710
	\bar{x}		0.6734	0.8711	0.8996	0.8917	2.3897
	s_N		0.0056	0.0069	0.0061	0.0052	0.0165
Tiny	(1234,1234)	3	0.5704	0.7628	0.9139	0.9080	2.1443
Tiny	(1234,2345)	3	0.5801	0.7654	0.9133	0.9072	2.1498
Tiny	(2345,1234)	3	0.5496	0.7156	0.9227	0.9189	2.0454
	\bar{x}		0.5667	0.7479	0.9166	0.9114	2.1132
	s_N		0.0156	0.0280	0.0052	0.0065	0.0587
Tiny	(1234,1234)	4	0.5688	0.6538	0.9165	0.9103	1.9229
Tiny	(1234,2345)	4	0.5612	0.6374	0.9190	0.9160	1.8915
Tiny	(2345,1234)	4	0.5771	0.6680	0.9246	0.9181	1.9503
	\bar{x}		0.5690	0.6531	0.9200	0.9148	1.9216
	s_N		0.0080	0.0153	0.0042	0.0040	0.0294
Tiny	(1234,1234)	5	0.5574	0.5760	0.9146	0.9100	1.7789
Tiny	(1234,2345)	5	0.5565	0.5820	0.9209	0.9155	1.7895
Tiny	(2345,1234)	5	0.5376	0.5589	0.9221	0.9168	1.7488
	\bar{x}		0.5505	0.5723	0.9192	0.9141	1.7724
	s_N		0.0111	0.0120	0.0040	0.0036	0.0211
Small	(1234,1234)	0	0.3026	0.7616	0.9209	0.9224	2.1418
Small	(1234,2345)	0	0.3007	0.7522	0.9247	0.9249	2.1217
Small	(2345,1234)	0	0.3009	0.7520	0.9210	0.9222	2.1211
	\bar{x}		0.3014	0.7553	0.9222	0.9232	2.1282
	s_N		0.0011	0.0055	0.0021	0.0015	0.0118
Small	(1234,1234)	1	0.2225	0.6476	0.9296	0.9293	1.9110
Small	(1234,2345)	1	0.2224	0.6332	0.9290	0.9282	1.8837
Small	(2345,1234)	1	0.2213	0.6311	0.9295	0.9314	1.8797
	\bar{x}		0.2221	0.6373	0.9294	0.9297	1.8915
	s_N		0.0007	0.0090	0.0003	0.0016	0.0171
Small	(1234,1234)	2	0.2083	0.4312	0.9328	0.9314	1.5391
Small	(1234,2345)	2	0.2055	0.4225	0.9352	0.9340	1.5258
Small	(2345,1234)	2	0.2069	0.4330	0.9360	0.9356	1.5419

Table 1: Variations of the pre-training performance of BERT versus dataset and model sizes (continued)

BERT Variant	(Model,Data) Seed	k^a	T-Loss \downarrow^d	V-Loss \downarrow^d	V-Acc \uparrow^d	V-wF1 \uparrow^d	V-PPPL \downarrow^d
	\bar{x}		0.2069	0.4289	0.9347	0.9337	1.5356
	s_N		0.0014	0.0056	0.0017	0.0021	0.0086
Small	(1234,1234)	3	0.1893	0.3779	0.9290	0.9306	1.4593
Small	(1234,2345)	3	0.1894	0.3766	0.9321	0.9325	1.4573
Small	(2345,1234)	3	0.1891	0.3722	0.9295	0.9299	1.4509
	\bar{x}		0.1893	0.3755	0.9302	0.9310	1.4558
	s_N		0.0002	0.0030	0.0017	0.0014	0.0044
Small	(1234,1234)	4	0.2085	0.3115	0.9402	0.9396	1.3654
Small	(1234,2345)	4	0.2078	0.3105	0.9346	0.9334	1.3641
Small	(2345,1234)	4	0.2077	0.3112	0.9341	0.9337	1.3651
	\bar{x}		0.2080	0.3111	0.9363	0.9356	1.3649
	s_N		0.0004	0.0005	0.0034	0.0035	0.0007
Small	(1234,1234)	5	0.2165	0.2611	0.9359	0.9358	1.2984
Small	(1234,2345)	5	0.2159	0.2601	0.9371	0.9369	1.2971
Small	(2345,1234)	5	0.2164	0.2609	0.9386	0.9392	1.2981
	\bar{x}		0.2163	0.2607	0.9372	0.9373	1.2979
	s_N		0.0003	0.0005	0.0014	0.0017	0.0007
Base^b	(1234,1234)	0	3.1122	3.1122	0.1504	0.0393	29.0734
Base	(1234,2345)	0	0.2275	0.6553	0.9284	0.9273	1.9257
Base^b	(2345,1234)	0	3.1113	3.3697	0.1600	0.0441	29.0711
	\bar{x}		2.1503	2.3791	0.4129	0.3369	20.0234
	s_N		1.6652	1.4984	0.4464	0.5113	15.6730
Base	(1234,1234)	1	0.1530	0.5360	0.9346	0.9331	1.7092
Base^b	(1234,2345)	1	3.1026	3.3638	0.1545	0.0414	28.8994
Base^b	(2345,1234)	1	3.0988	3.3586	0.1600	0.0441	28.7492
	\bar{x}		2.1181	2.4195	0.4164	0.3395	19.7859
	s_N		1.7019	1.6311	0.4488	0.5141	15.6551
Base	(1234,1234)	2	0.1461	0.3709	0.9371	0.9347	1.4490
Base	(1234,2345)	2	0.1476	0.3709	0.9408	0.9394	1.4490
Base	(2345,1234)	2	0.1457	0.3728	0.9386	0.9381	1.4518
	\bar{x}		0.1465	0.3715	0.9389	0.9374	1.4499
	s_N		0.0010	0.0011	0.0019	0.0024	0.0016
Base	(1234,1234)	3	0.1387	0.3295	0.9359	0.9354	1.3902
Base	(1234,2345)	3	0.1396	0.3310	0.9346	0.9347	1.3923
Base	(2345,1234)	3	0.1385	0.3299	0.9334	0.9334	1.3909
	\bar{x}		0.1390	0.3301	0.9346	0.9345	1.3911
	s_N		0.0006	0.0008	0.0012	0.0010	0.0011

Table 1: Variations of the pre-training performance of BERT versus dataset and model sizes (continued)

BERT Variant	(Model,Data) Seed	k^a	T-Loss \downarrow^d	V-Loss \downarrow^d	V-Acc \uparrow^d	V-wF1 \uparrow^d	V-PPPL \downarrow^d
Base	(1234,1234)	4	0.1580	0.2693	0.9446	0.9425	1.3091
Base	(1234,2345)	4	0.1584	0.2704	0.9384	0.9377	1.3105
Base^{b,c}	(2345,1234)	4	3.1273	4.5999	0.1390	0.0339	99.4766
	\bar{x}		0.1582	0.2699	0.9415	0.9401	1.3098
	s_N		0.0002	0.0008	0.0044	0.0034	0.0010
Base	(1234,1234)	5	0.1680	0.2168	0.9396	0.9395	1.2421
Base^{b,c}	(1234,2345)	5	0.8962	3.5788	0.1504	0.0393	35.8305
Base	(2345,1234)	5	0.1669	0.2174	0.9380	0.9379	1.2428
	\bar{x}		0.1675	0.2171	0.9388	0.9387	1.2425
	s_N		0.0008	0.0004	0.0011	0.0011	0.0005

^a The bin index, k , determines the number of samples in the training split.

^b The model diverges during training and/or stopped by the early stopping criterion.

^c The model is excluded from calculating the mean (\bar{x}) and standard deviation (s_N).

^d \uparrow : higher is better; \downarrow : lower is better.

4 Ablation Studies and Hyperparameter Tuning

4.1 Supervised fine-tuning on the Biogen ADME Dataset

The absorption, distribution, metabolism, and excretion (ADME) public dataset involves six *in vitro* ADME endpoints: human liver microsomal (HLM), rat liver microsomal (RLM), human plasma protein binding (hPPB), rat plasma protein binding (rPPB), MDR1-MDCK efflux ratio (MDR1-MDCK ER) and solubility.⁵ All SMILES are standardized using PubChem’s standardization protocol and tokenized using the WordPiece tokenizer. The dataset is randomly split into a training and testing subsets with a ratio of 80:20% within each property. The training set is further divided into 3 folds for cross-validation following hyperparameter optimization using grid search for classical machine learning (ML) models and Bayesian search for BERT models. The best performing model is selected based on the R^2 metric obtained from the cross-validation procedure. In addition to R^2 , we include

other regression performance metrics such as mean squared error (MSE), mean absolute error (MAE), root mean squared error (RMSE) and Pearson R for further analysis.

Tables 2-7 summarize the regression performance statistics of the Tiny-, Small- and Base-BERT as well as classical ML models, fine-tuned on Biogen’s ADME dataset. Numerical entries without parentheses correspond to the cross-validation results, summarized as $\bar{x} \pm s_N$. The test set performance metrics are presented as numerical entries within the parentheses.

Table 2: Supervised fine-tuning performance metrics obtained via 3-fold cross-validation hyperparameter optimization on Biogen’s public ADME dataset with experimental HLM data as labels^{a,b}

Models	MAE \downarrow^c	RMSE \downarrow^c	Pearson R \uparrow^c	R^2 \uparrow^c
Lasso Regression	0.403 \pm 0.006 (0.407)	0.498 \pm 0.007 (0.518)	0.602 \pm 0.010 (0.567)	0.360 \pm 0.012 (0.318)
Support Vector Machine	0.371 \pm 0.004 (0.356)	0.466 \pm 0.004 (0.452)	0.667 \pm 0.010 (0.696)	0.441 \pm 0.013 (0.479)
Random Forest	0.399 \pm 0.006 (0.385)	0.492 \pm 0.006 (0.483)	0.621 \pm 0.011 (0.641)	0.378 \pm 0.010 (0.406)
XGBoost	0.380 \pm 0.009 (0.377)	0.482 \pm 0.005 (0.489)	0.640 \pm 0.013 (0.640)	0.402 \pm 0.018 (0.392)
LightGBM	0.368 \pm 0.008 (0.366)	0.466 \pm 0.004 (0.472)	0.665 \pm 0.024 (0.661)	0.440 \pm 0.031 (0.434)
BERT-Tiny	0.441 \pm 0.017 (0.450)	0.545 \pm 0.009 (0.556)	0.495 \pm 0.033 (0.470)	0.224 \pm 0.042 (0.198)
BERT-Small	0.370 \pm 0.013 (0.354)	0.483 \pm 0.016 (0.471)	0.647 \pm 0.034 (0.672)	0.386 \pm 0.063 (0.418)
BERT-Base	0.354 \pm 0.004 (0.333)	0.454 \pm 0.004 (0.427)	0.681 \pm 0.021 (0.728)	0.453 \pm 0.038 (0.523)

^a The statistics are summarized as $\bar{x} \pm s_N$ where \bar{x} and s_N are the mean and standard deviation of the calculated metrics over the 3 cross-validation folds. The testing performance metrics (shown in parentheses) are obtained from refitting the best models on the entire training set and evaluating them on the test set.

^b The best test results are shown in boldface.

^c \uparrow : higher is better; \downarrow : lower is better.

Table 3: Supervised fine-tuning performance metrics obtained via 3-fold cross-validation hyperparameter optimization on Biogen’s public ADME dataset with experimental RLM data as labels^{a,b}

Models	MAE \downarrow^c	RMSE \downarrow^c	Pearson R \uparrow^c	R^2 \uparrow^c
Lasso Regression	0.442 \pm 0.010 (0.440)	0.558 \pm 0.011 (0.563)	0.676 \pm 0.017 (0.680)	0.445 \pm 0.021 (0.452)
Support Vector Machine	0.414 \pm 0.004 (0.416)	0.523 \pm 0.008 (0.535)	0.718 \pm 0.011 (0.714)	0.512 \pm 0.016 (0.505)
Random Forest	0.453 \pm 0.008 (0.454)	0.562 \pm 0.008 (0.568)	0.667 \pm 0.020 (0.669)	0.437 \pm 0.024 (0.442)
XGBoost	0.436 \pm 0.005 (0.431)	0.548 \pm 0.011 (0.553)	0.687 \pm 0.016 (0.693)	0.464 \pm 0.025 (0.471)
LightGBM	0.417 \pm 0.006 (0.409)	0.527 \pm 0.009 (0.532)	0.710 \pm 0.015 (0.715)	0.504 \pm 0.022 (0.511)
BERT-Tiny	0.498 \pm 0.007 (0.499)	0.626 \pm 0.011 (0.634)	0.560 \pm 0.023 (0.590)	0.272 \pm 0.037 (0.298)
BERT-Small	0.444 \pm 0.014 (0.437)	0.563 \pm 0.011 (0.562)	0.683 \pm 0.020 (0.707)	0.414 \pm 0.032 (0.446)
BERT-Base	0.411 \pm 0.013 (0.399)	0.528 \pm 0.016 (0.510)	0.716 \pm 0.019 (0.755)	0.496 \pm 0.034 (0.542)

^a The statistics are summarized as $\bar{x} \pm s_N$ where \bar{x} and s_N are the mean and standard deviation of the calculated metrics over the 3 cross-validation folds. The testing performance metrics (shown in parentheses) are obtained from refitting the best models on the entire training set and evaluating them on the test set.

^b The best test results are shown in boldface.

^c \uparrow : higher is better; \downarrow : lower is better.

Table 4: Supervised fine-tuning performance metrics obtained via 3-fold cross-validation hyperparameter optimization on Biogen’s public ADME dataset with experimental hPPB data as labels^{a,b}

Models	MAE ↓ ^c	RMSE ↓ ^c	Pearson R ↑ ^c	R ² ↑ ^c
Lasso Regression	0.387 ± 0.010 (0.410)	0.502 ± 0.013 (0.542)	0.721 ± 0.010 (0.686)	0.519 ± 0.015 (0.469)
Support Vector Machine	0.363 ± 0.014 (0.388)	0.479 ± 0.018 (0.536)	0.752 ± 0.010 (0.701)	0.562 ± 0.016 (0.481)
Random Forest	0.408 ± 0.015 (0.422)	0.523 ± 0.018 (0.548)	0.696 ± 0.019 (0.679)	0.477 ± 0.024 (0.458)
XGBoost	0.390 ± 0.005 (0.421)	0.509 ± 0.010 (0.547)	0.713 ± 0.006 (0.681)	0.505 ± 0.008 (0.459)
LightGBM	0.374 ± 0.010 (0.408)	0.491 ± 0.015 (0.529)	0.735 ± 0.008 (0.703)	0.539 ± 0.011 (0.494)
BERT-Tiny	0.464 ± 0.012 (0.494)	0.595 ± 0.017 (0.612)	0.573 ± 0.021 (0.564)	0.312 ± 0.015 (0.312)
BERT-Small	0.393 ± 0.012 (0.452)	0.507 ± 0.018 (0.601)	0.716 ± 0.013 (0.638)	0.495 ± 0.020 (0.344)
BERT-Base	0.372 ± 0.009 (0.409)	0.484 ± 0.007 (0.549)	0.741 ± 0.003 (0.688)	0.537 ± 0.008 (0.454)

^a The statistics are summarized as $\bar{x} \pm s_N$ where \bar{x} and s_N are the mean and standard deviation of the calculated metrics over the 3 cross-validation folds. The testing performance metrics (shown in parentheses) are obtained from refitting the best models on the entire training set and evaluating them on the test set.

^b The best test results are shown in boldface.

^c ↑: higher is better; ↓: lower is better.

Table 5: Supervised fine-tuning performance metrics obtained via 3-fold cross-validation hyperparameter optimization on Biogen’s public ADME dataset with experimental rPPB data as labels^{a,b}

Models	MAE ↓ ^c	RMSE ↓ ^c	Pearson R ↑ ^c	R ² ↑ ^c
Lasso Regression	0.430 ± 0.021 (0.416)	0.565 ± 0.032 (0.534)	0.681 ± 0.033 (0.697)	0.453 ± 0.044 (0.474)
Support Vector Machine	0.411 ± 0.014 (0.381)	0.550 ± 0.031 (0.512)	0.696 ± 0.029 (0.720)	0.481 ± 0.042 (0.516)
Random Forest	0.450 ± 0.017 (0.420)	0.576 ± 0.030 (0.529)	0.667 ± 0.042 (0.702)	0.430 ± 0.044 (0.484)
XGBoost	0.430 ± 0.014 (0.425)	0.570 ± 0.028 (0.543)	0.668 ± 0.026 (0.681)	0.443 ± 0.036 (0.457)
LightGBM	0.427 ± 0.019 (0.417)	0.558 ± 0.026 (0.548)	0.684 ± 0.024 (0.671)	0.466 ± 0.033 (0.447)
BERT-Tiny	0.525 ± 0.026 (0.514)	0.649 ± 0.040 (0.620)	0.531 ± 0.054 (0.560)	0.259 ± 0.062 (0.287)
BERT-Small	0.468 ± 0.043 (0.422)	0.601 ± 0.048 (0.558)	0.616 ± 0.047 (0.673)	0.363 ± 0.056 (0.422)
BERT-Base	0.435 ± 0.029 (0.401)	0.567 ± 0.032 (0.526)	0.670 ± 0.024 (0.700)	0.442 ± 0.036 (0.487)

^a The statistics are summarized as $\bar{x} \pm s_N$ where \bar{x} and s_N are the mean and standard deviation of the calculated metrics over the 3 cross-validation folds. The testing performance metrics (shown in parentheses) are obtained from refitting the best models on the entire training set and evaluating them on the test set.

^b The best test results are shown in boldface.

^c ↑: higher is better; ↓: lower is better.

Table 6: Supervised fine-tuning performance metrics obtained via 3-fold cross-validation hyperparameter optimization on Biogen’s public ADME dataset with experimental solubility data as labels^{a,b}

Models	MAE ↓ ^c	RMSE ↓ ^c	Pearson R ↑ ^c	R ² ↑ ^c
Lasso Regression	0.429 ± 0.015 (0.416)	0.574 ± 0.019 (0.569)	0.551 ± 0.002 (0.535)	0.290 ± 0.008 (0.282)
Support Vector Machine	0.414 ± 0.020 (0.390)	0.565 ± 0.025 (0.551)	0.569 ± 0.010 (0.572)	0.313 ± 0.014 (0.326)
Random Forest	0.416 ± 0.010 (0.388)	0.575 ± 0.021 (0.558)	0.553 ± 0.011 (0.565)	0.289 ± 0.006 (0.310)
XGBoost	0.413 ± 0.005 (0.404)	0.584 ± 0.010 (0.593)	0.532 ± 0.020 (0.497)	0.264 ± 0.033 (0.221)
LightGBM	0.394 ± 0.008 (0.371)	0.563 ± 0.014 (0.549)	0.571 ± 0.026 (0.577)	0.316 ± 0.031 (0.331)
BERT-Tiny	0.424 ± 0.020 (0.403)	0.592 ± 0.029 (0.594)	0.490 ± 0.022 (0.467)	0.231 ± 0.019 (0.209)
BERT-Small	0.390 ± 0.040 (0.360)	0.550 ± 0.036 (0.562)	0.594 ± 0.039 (0.563)	0.341 ± 0.039 (0.290)
BERT-Base	0.390 ± 0.040 (0.342)	0.559 ± 0.038 (0.529)	0.578 ± 0.026 (0.627)	0.322 ± 0.035 (0.376)

^a The statistics are summarized as $\bar{x} \pm s_N$ where \bar{x} and s_N are the mean and standard deviation of the calculated metrics over the 3 cross-validation folds. The testing performance metrics (shown in parentheses) are obtained from refitting the best models on the entire training set and evaluating them on the test set.

^b The best test results are shown in boldface.

^c ↑: higher is better; ↓: lower is better.

Table 7: Supervised fine-tuning performance metrics obtained via 3-fold cross-validation hyperparameter optimization on Biogen’s public ADME dataset with experimental MDR1-ER data as labels^{a,b}

Models	MAE ↓ ^c	RMSE ↓ ^c	Pearson R ↑ ^c	R ² ↑ ^c
Lasso Regression	0.373 ± 0.007 (0.383)	0.485 ± 0.008 (0.516)	0.708 ± 0.010 (0.677)	0.499 ± 0.014 (0.458)
Support Vector Machine	0.341 ± 0.008 (0.338)	0.457 ± 0.011 (0.476)	0.747 ± 0.013 (0.736)	0.555 ± 0.018 (0.539)
Random Forest	0.390 ± 0.007 (0.386)	0.502 ± 0.004 (0.502)	0.686 ± 0.008 (0.709)	0.462 ± 0.011 (0.488)
XGBoost	0.359 ± 0.005 (0.351)	0.480 ± 0.006 (0.482)	0.716 ± 0.010 (0.728)	0.510 ± 0.013 (0.527)
LightGBM	0.353 ± 0.005 (0.340)	0.469 ± 0.006 (0.471)	0.730 ± 0.007 (0.742)	0.531 ± 0.009 (0.549)
BERT-Tiny	0.408 ± 0.008 (0.402)	0.539 ± 0.016 (0.541)	0.622 ± 0.025 (0.640)	0.376 ± 0.035 (0.393)
BERT-Small	0.365 ± 0.007 (0.386)	0.486 ± 0.012 (0.511)	0.711 ± 0.013 (0.693)	0.489 ± 0.034 (0.457)
BERT-Base	0.341 ± 0.015 (0.319)	0.457 ± 0.022 (0.448)	0.744 ± 0.020 (0.772)	0.535 ± 0.026 (0.583)

^a The statistics are summarized as $\bar{x} \pm s_N$ where \bar{x} and s_N are the mean and standard deviation of the calculated metrics over the 3 cross-validation folds. The testing performance metrics (shown in parentheses) are obtained from refitting the best models on the entire training set and evaluating them on the test set.

^b The best test results are shown in boldface.

^c ↑: higher is better; ↓: lower is better.

4.2 Hyperparameter Search Spaces for Classical ML Models

The pre-defined search space for the hyperparameter optimization of the classical ML on Biogen’s ADME dataset is provided in Table 8 which closely follows that of Ref. 5.

Table 8: Pre-defined search space for grid-search hyperparameter optimization of classical machine learning models performed over ADME dataset^a

Model	Parameter	Allowed Values
BERT	stack_depth	{0, 1, 2, 3, 4, 5}
	p	{0.0, 0.1, 0.2, 0.3, 0.4, 0.5}
	batch_size	{8, 16, 32, 64, 128, 256, 512}
	learning_rate	{1E-06, 1E-05, 5E-05, 1E-04, 5E-04, 1E-03}
	weight_decay	{0.0, 1E-04, 5E-04, 1E-03, 5E-03, 1E-02, 5E-02, 1E-01}
	freeze_base_model	{True, False}
LASSO	LASSO__alpha	{0.001, 0.005, 0.01, 0.05, 0.1, 0.5, 1.0, 2.0, 5.0}
SVM	SVM__C	{0.1, 1.0, 5.0, 10.0, 20.0, 50.0}
	SVM__epsilon	{0.01, 0.1, 0.3, 0.5}
	SVM__gamma	{"scale", "auto"}
RF	max_depth	{15, 25, 40, None}
	max_features	{"sqrt", 0.33, 0.67, None}
	n_estimators	{100, 250, 500, 750, 1000}
XGBoost ^b	n_estimators (Round 1)	{100, 250, 500, 750, 1000}
	max_depth (Round 2)	{3, 4, 5, 6, 7}
	min_child_weight (Round 2)	{1, 2, 3}
	gamma (Round 3)	{0.0, 0.05, 0.1}
	subsample (Round 4)	{0.6, 0.7, 0.8, 0.9, 1.0}
	colsample_bytree (Round 4)	{0.6, 0.7, 0.8, 0.9, 1.0}
	reg_alpha (Round 5)	{0.0, 0.1, 0.2, 0.3, 0.4}
reg_lambda (Round 5)	{1.0, 1.1, 1.2, 1.3, 1.4}	
LightGBM ^c	n_estimators (Round 1)	{100, 250, 500, 750, 1000}
	num_leaves (Round 2)	{15, 31, 45, 60, 75}
	min_child_samples (Round 2)	{10, 20, 30, 40}
	subsample (Round 3)	{0.6, 0.7, 0.8, 0.9, 1.0}
	colsample_bytree (Round 3)	{0.6, 0.7, 0.8, 0.9, 1.0}
	subsample_freq (Round 3)	{1, 2, 3, 5}
	reg_alpha (Round 4)	{0.0, 0.2, 0.5, 0.8}
	reg_lambda (Round 4)	{0.0, 0.2, 0.5, 0.8}

^a In order to reduce the computational cost of hyperparameter optimization, we followed Ref. 5 and performed a multi-step grid-search optimization for the XGBoost and LightGBM models. In each round of the grid-search, we optimized a subset of the total set of hyperparameters while keeping the rest of the hyperparameters fixed.

^b Initial parameters were set to: n_estimators = 500; subsample = 0.8; colsample_bytree = 0.8; random_state = 1234.

^c Initial parameters were set to: n_estimators = 500; subsample = 0.8; colsample_bytree = 0.8; subsample_freq = 1; random_state = 1234.

4.3 Optimized Hyperparameters of the Fine-tuned Models

Tables 9–14 provide a complete list of optimized hyperparameters for all fine-tuned models considered in this study.

Table 9: Optimized parameters for the LASSO model obtained from grid-search hyperparameter optimization with 3-fold cross-validation using ADME dataset

Parameter	Target Property					
	HLM	RLM	hPPB	rPPB	SOL	MDR1-ER
LASSO__alpha	0.005	0.001	0.005	0.005	0.005	0.005

Table 10: Optimized hyperparameters for the support vector machine model obtained from grid-search hyperparameter optimization with 3-fold cross-validation using ADME dataset

Parameter	Target Property					
	HLM	RLM	hPPB	rPPB	SOL	MDR1-ER
SVM__C	5	5	10	5	5	5
SVM__epsilon	0.1	0.1	0.1	0.1	0.3	0.1
SVM__gamma	“scale”	“auto”	“auto”	“auto”	“auto”	“auto”

Table 11: Optimized hyperparameters for the random forest model obtained from grid-search hyperparameter optimization with 3-fold cross-validation using ADME dataset

Parameter	Target Property					
	HLM	RLM	hPPB	rPPB	SOL	MDR1-ER
max_depth	15	40	25	25	None	None
max_features	0.67	None	0.67	0.67	0.33	0.67
n_estimators	750	500	1000	1000	500	1000

Table 12: Optimized hyperparameters for the XGBoost model obtained from grid-search hyperparameter optimization with 3-fold cross-validation using ADME dataset^{a,b}

Parameter	Target Property					
	HLM	RLM	hPPB	rPPB	SOL	MDR1-ER
n_estimators (Round 1)	750	750	100	100	750	1000
max_depth (Round 2)	3	3	3	3	5	4
min_child_weight (Round 2)	1	2	2	2	2	1
gamma (Round 3)	0.0	0.0	0.0	0.0	0.0	0.1
colsample_bytree (Round 4)	0.8	0.9	0.7	0.9	0.6	0.6
subsample (Round 4)	0.9	0.9	0.9	1.0	1.0	1.0
reg_alpha (Round 5)	0.3	0.1	0.0	0.1	0.1	0.1
reg_lambda (Round 5)	1.4	1.0	1.0	1.0	1.2	1.3

^a In order to reduce the computational cost of hyperparameter optimization, we followed Ref. 5 and performed a multi-step grid-search optimization for the XGBoost. In each round of the grid-search, we optimized a subset of the total set of hyperparameters while keeping the rest of the hyperparameters fixed to their initial values.

^b Initial parameters were set to: n_estimators = 500; subsample = 0.8; colsample_bytree = 0.8; random_state = 1234.

Table 13: Optimized hyperparameters for the LightGBM model obtained from grid-search hyperparameter optimization with 3-fold cross-validation using ADME dataset^{a,b}

Parameter	Target Property					
	HLM	RLM	hPPB	rPPB	SOL	MDR1-ER
n_estimators (Round 1)	1000	750	1000	100	500	100
min_child_samples (Round 2)	40	10	20	10	10	20
num_leaves (Round 2)	75	15	15	15	15	15
colsample_bytree (Round 3)	0.9	1.0	0.6	0.8	1.0	0.8
subsample (Round 3)	0.8	0.9	0.9	0.8	0.9	1.0
subsample_freq (Round 3)	3	1	1	5	1	3
reg_alpha (Round 4)	0.2	0.0	0.0	0.2	0.0	0.0
reg_lambda (Round 4)	0.5	0.0	0.0	0.5	0.0	0.0

^a In order to reduce the computational cost of hyperparameter optimization, we followed Ref. 5 and performed a multi-step grid-search optimization for the LightGBM. In each round of the grid-search, we optimized a subset of the total set of hyperparameters while keeping the rest of the hyperparameters fixed to their initial values.

^b Initial parameters were set to: n_estimators = 500; subsample = 0.8; colsample_bytree = 0.8; subsample_freq = 1; random_state = 1234.

Table 14: Optimized hyperparameters for different variants of BERT model obtained from conducting Bayesian search hyperparameter optimization with 3-fold cross-validation over ADME dataset

Model	Parameter	Target Property					
		HLM	RLM	hPPB	rPPB	SOL	MDR1-ER
Tiny-BERT	stack_depth	5	1	5	5	1	2
	p	0.3	0.4	0.0	0.4	0.4	0.5
	batch_size	128	256	128	64	64	128
	learning_rate	5E-04	1E-04	5E-05	1E-04	5E-05	5E-05
	weight_decay	0.05	0.00	0.01	0.1	0.0001	0.01
	freeze_base_model	True	False	False	False	False	False
Small-BERT	stack_depth	0	1	3	5	3	3
	p	0.5	0.3	0.2	0.3	0.4	0.4
	batch_size	64	32	128	64	64	256
	learning_rate	1E-04	5E-05	1E-04	1E-04	1E-03	1E-03
	weight_decay	0.1	0.0005	0.01	0.0005	0.001	0.0005
	freeze_base_model	False	False	False	False	True	True
Base-BERT	stack_depth	0	2	3	4	3	0
	p	0.3	0.2	0.2	0.4	0.5	0.3
	batch_size	128	64	256	128	512	32
	learning_rate	5E-05	5E-05	1E-04	1E-04	1E-03	1E-04
	weight_decay	0.0005	0.1	0.0005	0.1	0.1	0.0005
	freeze_base_model	False	False	False	False	True	False

5 Budget and Cost Estimations

In this section, we offer an estimated list of costs associated with pre-training and fine-tuning BERT. Using Table 15, one can estimate the pre-training and evaluation cost of Base-BERT on the PubChem dataset for 10 epochs with a global batch size of 1024 on an AWS `p5en.48xlarge` instance with 8 NVIDIA H200 GPUs to be around \$10,000 for roughly 6.5 days. Similarly, the total cost of pre-training and evaluation of Small-BERT on two `g6e.12xlarge` nodes with a total of 8 NVIDIA L40S GPUs is about \$2,700 for 5.3 days. Finally, pre-training and evaluation of Tiny-BERT takes about 2.3 days on 4 nodes with a total of 16 NVIDIA A30 GPUs. The corresponding cost on AWS with four `g6e.12xlarge` instances, assuming that the total runtime remains the same, is around \$2,300. On the other hand, the entire 3-fold cross-validation hyperparameter search on the same dataset, using the support vector machine (SVM) model, can be completed in a few minutes on a personal multi-core CPU computer. Pre-training 160 BERT models and their subsequent fine-tunings took us about 18 months on a university-wide shared supercomputing cluster as a consistent and airtight implementation of the experiments across partitions with carefully controlled environment was the only viable option for us to enable a meaningful and systematic exploration in our study. We hope releasing all our codes, scripts, data and model artifacts to the public can facilitate transparency and reproducibility of our experiments and enable further research in this area.

Table 15: Estimated costs required for pre-training BERT models on the entire PubChem (version 4-18-2025) dataset

Instance Name	vCPU Count	GPU Types	On-demand Price (\$/h) ^a	GPU Memory (GB)	Instance Memory (GB)	Instance Storage (GB)
<code>p5en.48xlarge</code>	192	8 × H200	63.30	8 × 141 (HBM3e)	2048	8 × 3840 NVMe SSD
<code>p4de.24xlarge</code>	96	8 × A100	27.45	8 × 80 (HBM2e)	1152	8 × 1000 NVMe SSD
<code>g6e.12xlarge</code>	48	4 × L40S	10.49	4 × 48	384	2 × 1900 NVMe SSD

^a On-demand prices are based on per-instance-hour and are obtained from AWS website (<https://aws.amazon.com/ec2/pricing/on-demand>) on 03/03/2026 and are intended for illustrative purposes only. Prices may vary based on the region, availability, and other factors.

6 BERT Architectural Details

Table 16 provides the architectural details of Tiny-, Small- and Base-BERT model variants.

Table 16: Architectural details of different BERT model variants

Model Details	BERT Variant		
	Tiny	Small	Base
Hidden Size	128	512	768
Hidden Activation	GELU	GELU	GELU
Vocabulary Size	30522	30522	30522
Max Position Embeddings	512	512	512
Intermediate Size	512	2048	3072
Hidden Dropout Probability	0.1	0.1	0.1
Attention Dropout Probability	0.1	0.1	0.1
# Hidden Layers	2	4	12
# Attention Heads	2	8	12
# Parameters (M)	4.4	28.5	108

References

- (1) Landrum, Greg RDKit: Open-Source Cheminformatics Software. 2006; <http://www.rdkit.org>, 2025_03_3 (Q1 2025) Release; DOI: <https://doi.org/10.5281/zenodo.15605628>.
- (2) Bento, A. P.; Hersey, A.; Félix, E.; Landrum, G.; Gaulton, A.; Atkinson, F.; Bellis, L. J.; Veij, M. D.; Leach, A. R. An open source chemical structure curation pipeline using RDKit. *Journal of Cheminformatics* **2020**, *12*, 51.
- (3) Hähnke, V. D.; Kim, S.; Bolton, E. E. PubChem chemical structure standardization. *Journal of Cheminformatics* **2018**, *10*, 36.
- (4) Carcinogenic Potency Database (CPDB) Summary Table by Chemical of the Carcinogenic Potency Database. 2025; <https://files.toxplanet.com/cpdb>, <https://files.toxplanet.com/cpdb/chemicalsummary.html>; (last accessed: 09/29/2025).
- (5) Fang, C.; Wang, Y.; Grater, R.; Kapadnis, S.; Black, C.; Trapa, P.; Sciabola, S. Prospective Validation of Machine Learning Algorithms for Absorption, Distribution, Metabolism, and Excretion Prediction: An Industrial Perspective. *Journal of Chemical Information and Modeling* **2023**, *63*, 3263–3274.